MASTERARBEIT | MASTER'S THESIS

Titel | Title

The development of the skeletomusculature in the sea spider Pycnogonum litorale (Strøm, 1762)
-with first insight into chelicerate myogenesis at the cellular level

verfasst von | submitted by
Max Hämmerle BSc

angestrebter akademischer Grad | in partial fulfilment of the requirements for the degree of
Master of Science (MSc)

Wien | Vienna, 2024

Studienkennzahl lt. Studienblatt | Degree programme code as it appears on the student record sheet:	UA 066 831
Studienrichtung lt. Studienblatt | Degree programme as it appears on the student record sheet:	Masterstudium Zoologie
Betreut von | Supervisor:	Dr. Georg Brenneis

Acknowledgements

First and foremost, I would like to thank my supervisor, Dr. Georg Brenneis for introducing me to the fascinating world of Pycnogonids and for his invaluable support throughout my thesis project, patiently answering my numerous questions and sharing his expertise on the methods employed.

I extend my gratitude to Univ.-Prof. DDr. Andreas Wanninger and Univ.-Prof. Mag. Dr. Mihaela Pavličev, the heads of the Department of Evolutionary Biology at the University of Vienna, for providing access to the facilities and resources that were necessary for the research presented in this thesis. I also want to thank the staff of the department for their advice and help on many occasions.

Special thanks go to:

Mag. Marion Wanninger for showing me the ropes in the Aqua Lab and helping with the animal cultivation.

Gudrun Schwarze MSc for keeping me company in the Imaging Lab during long hours of image reconstruction and for advice concerning the used colour schemes.

Antonia Grausgruber MSc for her company, advice and support throughout the work on my master thesis.

I would like to express my gratitude to my family for their continuous support throughout my academic journey and for providing me with the opportunity to study a subject that truly excites me.

Last but not least, I thank my friends and my partner Mag. Viktoria Thaller for their unending support and patience.

Abstract

Pycnogonids, as the sister group to all other Chelicerata, have the potential to provide unique insights into arthropod evolution. In recent years, the development of the pycnogonid species *Pycnogonum litorale* (Strøm, 1762) was studied in more detail, providing new insight in their anamorphic phase of development. This, for arthropods probably ancestral, developmental mode is characterised by the addition of new body segments and walking legs with each molt. However, the developmental process of myogenesis (muscle formation) remains so far unexplored. Indeed, studies on arthropod myogenesis at the cell level are generally scarce, outside of insects and some crustacean taxa. The “founder cell model” of myogenesis in the fruit fly *Drosophila melanogaster* describes how mononucleated founder cells fuse with myoblasts to form multinucleated muscle precursors. Similar processes where recently discovered in crustacean taxa. However, due to the lack of comparable data on myogenesis for Chelicerata and Myriapoda, it is unclear whether these patterns are representative of all arthropods. This study aimed to describe myogenetic patterns in *P. litorale* during its anamorphic development, focusing on muscle formation hot-spots like the walking legs, trunk musculature, and proctodeal dilator muscles. Additionally, changes in the proboscis musculature were explored, being predicted to occur with an obligatory feeding host shift from hydrozoans to sea anemones during *P. litorale* development. Using fluorescent histochemistry and immunohistochemistry to analyze myosin heavy chain and F-actin proteins, as well as HCR-FISH to study the expression patterns of myosin heavy chain (striated type 2) and the transcription factor myocyte-enhancer-factor 2 (MEF2), the study reveals new muscle structures and sequences of muscle formation. For the first time in a chelicerate, mononucleated muscle pioneer cells are identified, which were observed to differentiate into singular, seemingly multinucleated muscle fibers, reminiscent of the founder cell model. However, myoblast fusion, as well as multinucleated muscle precursor cells could not be conclusively documented. Muscle cells in *P. litorale* appear to remain mononucleated for an extended period before undergoing rapid nuclear addition to form multinucleated muscle fibers. This work contributes new insights into pycnogonid myogenesis and its potential relevance to broader arthropod developmental processes.

Zusammenfassung

Pycnogonida haben als die Schwestergruppe aller anderen Chelicerata das Potenzial einzigartige Einblicke in die Evolution der Arthropoden zu geben. In den letzten Jahren erbrachte die Erforschung der Entwicklung der Pycnogonidenart *Pycnogonum litorale* (Strøm, 1762) neue Erkenntnisse über ihre anamorphe Entwicklungsphase. Dieser für Gliederfüßer wahrscheinlich ursprüngliche Entwicklungsmodus ist dadurch gekennzeichnet, dass bei jeder Häutung neue Körpersegmente und Laufbeine hinzugefügt werden. Der Prozess der Myogenese (Muskelbildung) von Pycnogoniden ist jedoch bislang unerforscht. Abgesehen von Insekten und einigen Krebstieren sind Studien zur Myogenese von Arthropoden auf Zellebene allgemein selten. Das „Foundercell model (Gründerzellenmodell)“ der Myogenese der Fruchtfliege *Drosophila melanogaster* beschreibt, wie einkernige Gründerzellen mit Myoblasten fusionieren um mehrkernige Muskelvorläufer zu bilden. Ähnliche Prozesse wurden kürzlich bei Crustacea entdeckt. Da jedoch keine vergleichbaren Daten zur Myogenese bei Chelicerata und Myriapoda vorliegen, ist unklar, ob diese Muster für alle Arthropoden repräsentativ sind. Ziel dieser Masterarbeit war es, die myogenetischen Muster von *P. litorale* während der anamorphen Entwicklung zu beschreiben. Dabei lag der Schwerpunkt auf Hotspots der Muskelbildung, wie den Laufbeinen, der Rumpfmuskulatur und den proktodealen Dilatatormuskeln. Darüber hinaus wurden Veränderungen in der Rüsselmuskulatur untersucht, die mit einem Wechsel des Nahrungswirts von Hydrozoen zu Seeanemonen während der Entwicklung von *P. litorale* einhergehen. Mit Hilfe von Fluoreszenzhistochemie und Immunhistochemie zur Analyse von Myosin-Heavy-Chain- und F-Aktin-Proteinen, sowie HCR-FISH zur Untersuchung der Expressionsmuster von Myosin-Heavy-Chain (quergestreifter Typ 2) und des Transkriptionsfaktors Myocyte-enhancer-factor 2 (MEF2), zeigt die Studie neue Muskelstrukturen und Abläufe der Muskelbildung. Zum ersten Mal werden in einem Chelicerata einkernige Muskelpionierzellen identifiziert, die sich in einzelne, scheinbar vielkernige Muskelfasern differenzieren; dies erinnert an das „Founder cell model“. Eine Myoblastenfusion sowie mehrkernige Muskelvorläuferzellen konnten jedoch nicht schlüssig dokumentiert werden. Die Muskelzellen in *P. litorale* scheinen über einen längeren Zeitraum mononukleiert zu bleiben, bevor sie durch rasche Kernaddition multinukleierte Muskelfasern bilden. Diese Arbeit trägt zu neuen Erkenntnissen über die Myogenese der Pycnogoniden und ihre potenzielle Bedeutung für weitreichendere Entwicklungsprozesse bei Arthropoden bei.

Index

Introduction 6

The anamorphic development of *P. litorale* 8

Thesis aim and research questions 11

Materials and Methods 13

Animal Cultivation 13

Staining reagents, buffers and solutions used during experimentation 13

Specimen fixation and storage 14

Pretreatments and specimen dissection 14

Fluorescent histochemistry and immunohistochemistry (IHC) 15

Hybridization chain reaction RNA-fluorescent in-situ hybridization (HCR-FISH) 16

Mounting of samples 18

Data documentation and visualization 18

Selection of terminology 19

Results 21

Differential staining characteristics of protein labelling and candidate gene expression 21

Sequence of muscle development and the folding of the leg within the limb bud 23

Musculature of the walking legs and their development outside the limb buds 26

Sequence of longitudinal trunk muscle development and description of a new muscle group 31

The development of the anus musculature and its division in two distinct muscle groups 33

The development of proboscis musculature from instar II to early stages of instar V 35

The remodelling of the proboscis and its musculature during instar V 39

The remodelled proboscis musculature of instar VI 41

Discussion 47

The configuration and developmental sequence of the limb bud musculature and formation of the walking legs 47

The myogenetic pattern of the asymmetrical developing longitudinal trunk musculature and the discovery of the secondary longitudinal muscles 48

Formation of anus dilator muscles and conformation of two distinct muscle groups 49

New insights into the development of the proboscis muscles and the remodelling of the pharyngeal suction pump 49

A clue to the founder cell model in Pycnogonida? 54

References 58

Appedices 62

Appendix 1: Buffers and solutions and their ingredients used in the experiments. 62

Appendix 2: Details on the staining reagents and mounting media used for fluorescent histochemistry, immunohistochemistry (IHC) and hybridization chain reaction RNA-fluorescent in-situ hybridization (HCR-FISH). 63

Appendix 3: Staining experiments and the staining reagents used. 64

Appendix 4: Sequences of the used probe pairs during HCR-FISH for the detection of myosin heavy chain (striated type 2) (MHCst) gene expression. 65

Appendix 5: Sequences of the used probe pairs during HCR-FISH for the detection of myocyte-enhancer-factor 2 (MEF2) gene expression. 66

Introduction

To uncover developmental processes and their evolutionary implications within the unparalleled diversity of Arthropoda has long been the task of many dedicated researchers. With the sheer amount of arthropod lineages, it is not surprising that some interesting taxa, in terms of morphology and development as well as phylogeny have not been studied in as much detail as others.

One of them are the Pycnogonida, also called sea spiders or Pantopoda. The term “Pantopoda”, which means “all feet”, already implies their bizarre morphology, which is mainly characterized by their typically 8 long segmented legs, which are attached to a reduced tube-like body (King 1973; Dencker 1974; Schram and Hedgpeth 1978). Another feature all pycnogonids share is a prominent proboscis, located at the cephalosoma (the anterior “head” segment) as feeding apparatus and a reduced unsegmented anal tubercle at the posterior body end (Fry 1965; King 1973; Fahrenbach and Arango 2007; Wagner et al. 2017; Dietz et al. 2018). Additional anterior located appendages, the claw-like cheliphores, the elongated palps and ovigers are species-dependently present or reduced in adult pycnogonids (Brenneis et al. 2017). Most pycnogonids hatch as a free-living, externally unsegmented protonymphon larva (Meisenheimer 1902; Behrens 1984; Alexeeva et al. 2017; Brenneis et al. 2017). This larva is the first instar of a so-called hemianamorphic postembryonic development (Alexeeva et al. 2017; Brenneis et al. 2017). This mode of development is split into an anamorphic phase, where new body segments emerge with each molt, and a subsequent epimorphic phase, where no additional segments are acquired but body growth happens with each molt.

Apart from their fascinating morphology and development also their phylogenetic position within the Chelicerata (sea spiders, horseshoe crabs and arachnids) make pycnogonids interesting study organisms for the uncovering of evolutionary processes within the arthropod lineage (Hedgpeth 1947; Giribet and Edgecombe 2019). Pycnogonids are the sister group to all other chelicerate taxa (Euchelicerata), from which they diverged already in the early Cambrian, near the base of the arthropod tree of life (Giribet and Edgecombe 2019).

Although pycnogonids have fascinated zoologists for over two and a half centuries and in recent years studies on their development have increased (Behrens 1984; Tomaschko et al. 1997; Vilpoux and Waloszek 2003; Brenneis et al. 2017; Alexeeva and Tamberg 2021), there remains a significant gap in our understanding of their postembryonic development in terms of myogenesis, the formation and development of musculature. More than a century ago, the skeletomusculature of the protonymphon larva of *Achelia echinata* Hodge, 1864 was described

(Meisenheimer 1902) and since then, only one other study has focused on the musculature of the same developmental stage in *Nymphon brevirostre* Hodge, 1863 (Alexeeva et al. 2017). Apart from this, available descriptions relate exclusively to the adult skeletomusculature (Fry 1965; Dencker 1974; Schram and Hedgpeth 1978; Tjønneland et al. 1985; Totland and Kryvi 1986; Fahrenbach 1994; Fahrenbach and Arango 2007; Wagner et al. 2017; Petrova and Bogomolova 2023). The fine structure of the heart (Tjønneland et al. 1985) and the somatic muscles (Totland and Kryvi 1986) of adult pycnogonids, have also been the subject of previous studies. Subsequently, Fahrenbach (1994) provided a supplemented summary to these findings, concluding that the skeletal musculature of pycnogonids is composed of individual striated muscle fibers (myofibers).

When it comes to modern data on myogenesis at the cellular level (i.e., how first progenitor muscle cells are formed and differentiate during development), data is not only non-existent for Pycnogonida but for Chelicerata in general. In fact, this kind of data are scarce in most arthropod groups. Among the two major arthropod taxa, Chelicerata and Mandibulata (centipedes, millipedes, crustaceans and insects), myogenesis is best understood in insects, where studies on the fruit fly *Drosophila melanogaster* resulted in the establishment of the so-called founder-cell model: mesodermal progenitor cells generate mononucleated founder cells through mitosis. These founder cells initiate the formation of multinucleate syncytial muscle precursors via cell fusion with neighbouring undifferentiated myoblasts (Bate 1990; Rushton et al. 1995; Gunage et al. 2017; Baylies, Bate, and Gomez 1998; Schröter et al. 2004; Abmayr and Pavlath 2012; Campos-Ortega and Hartenstein 2013). The precursors differentiate without further divisions into striated myofibers, which in *Drosophila* develop to single muscles, in contrast to vertebrates where bundles of myofibers form the skeletomusculature (Gunage et al. 2017; Chal and Pourquié 2017). Outside of insects, first investigations on crustaceans suggest similar myogenetic processes as in *Drosophila* (Kreissl, Uber, and Harzsch 2008; Harzsch and Kreissl 2010; Jirikowski et al. 2010; Jirikowski, Richter, and Wolff 2013), hinting toward a conserved pattern in the Pancrustacea (crustaceans + Hexapoda). However, due to the lack of comparable cell-level data on myogenesis in Chelicerata and Myriapoda, it is unclear whether the cell types and processes of insect and crustacean myogenesis are representative of the pancrustacean lineage only, or may be shared by all mandibulates, or potentially even all arthropods.

The above-mentioned lack of data led to the decision to study myogenesis in pycnogonids in this thesis. To uncover the muscle formation of pycnogonids during their postembryonic

development, and therefore lay the foundation for deeper inquiries on myogenesis at the cellular level, *Pycnogonum litorale* (Strøm, 1762) was chosen as study organism. In comparison to other pycnogonids, this species has rather short and thick legs, which insert in a compressed trunk. Their proboscis is cone-shaped and tapers at the end. Besides their first walking leg pair, the cephalosoma of adult males of *P. litorale* bear ovigers for the carrying of egg batches. In both sexes, the cheliphores are lost during development and the palps are completely missing (Behrens 1984; Vilpoux and Waloszek 2003; Alexeeva and Tamberg 2021).

P. litorale is distributed in the northern Atlantic, from the east coast of north America to the west coast of Europe, around Britain, in the North and Norwegian sea and even in the Arctic, inhabiting the littoral. *P. litorale* can be described as an ectoparasite, spending most of its time next to its cnidarian prey, feeding (Schmidt and Bückmann 1971). It displays a postembryonic hemianamoprhic development, typical for pycnogonids. At the end of its anamorphic developmental phase, a host shift occurs, whereby the larvae initially prey on a hydrozoan host from instar I to V, before switching to a sea anemone host at instar VI (Schmidt and Bückmann 1971; Behrens 1984; Vilpoux and Waloszek 2003; Alexeeva and Tamberg 2021).

The latest histological study on *P. litorale* development presented new insights into its internal organogenesis (Alexeeva and Tamberg 2021). Data on muscle development are completely missing in this work, and also in older studies information is scarce.

What makes *P. litorale* an ideal choice of study organism to address the lack of knowledge regarding pycnogonid myogenesis, is the fact that it can be cultured in the laboratory (Alexeeva and Tamberg 2021; Brenneis et al. 2023) and that detailed descriptions of its developmental stages are available (Behrens 1984; Tomaschko et al. 1997; Wilhelm et al. 1997; Brenneis et al. 2017a; Alexeeva et al. 2019; Alexeeva and Tamberg 2021; Vilpoux and Waloszek 2003).

The anamorphic development of *P. litorale*

The development of *P. litorale* can be divided into three phases. The larval phase consists of two protonymphon-like larval instars. These externally unsegmented larvae have a dorsomedian pair of eyes, a proboscis, a pair of larval cheliphores with elongated attachment gland spine and two pairs of larval legs (Fig. 1). This larval phase is followed by the postlarval phase (instars III-VI), which encompasses a series of anamorphic molts, during which new body segments and walking legs emerge (Fig. 1), followed by the juvenile phase characterized by body growth (Behrens 1984; Tomaschko et al. 1997; Vilpoux and Waloszek 2003; Brenneis et al. 2017a; Alexeeva and Tamberg 2021). Throughout the postlarval phase, a pair of limb buds can be discerned at the posterior end of the instars' body. With the maturation of an instar, the

prospective leg pair develops within them and emerges with the molt to the following instar as functioning pair of articulated legs (Tomaschko et al. 1997; Vilpoux and Waloszek 2003; Alexeeva and Tamberg 2021; Behrens 1984). Within the limb buds, however, the developmental sequence of future muscles as well as the configuration of the folding of the walking leg is until now unknown. By contrast, the external podomere development, is well documented (Vilpoux and Waloszek 2003; Alexeeva and Tamberg 2021; Behrens 1984). The first walking leg pair emerges at instar IV. Each leg consists of seven podomeres (coxa1, coxa2, coxa3, femur-patella complex, tibia, tarsus-propodus complex and the main claw). With the molt to instar V, the first walking legs gain an additional podomere through the division of the femur-patella complex into the definitive femur and patella, and the second walking leg emerges, consisting again of seven podomeres. At instar VI, the first walking leg has acquired the final nine-articled composition through the division of the penultimate tarsus-propodus complex into tarsus and propodus.

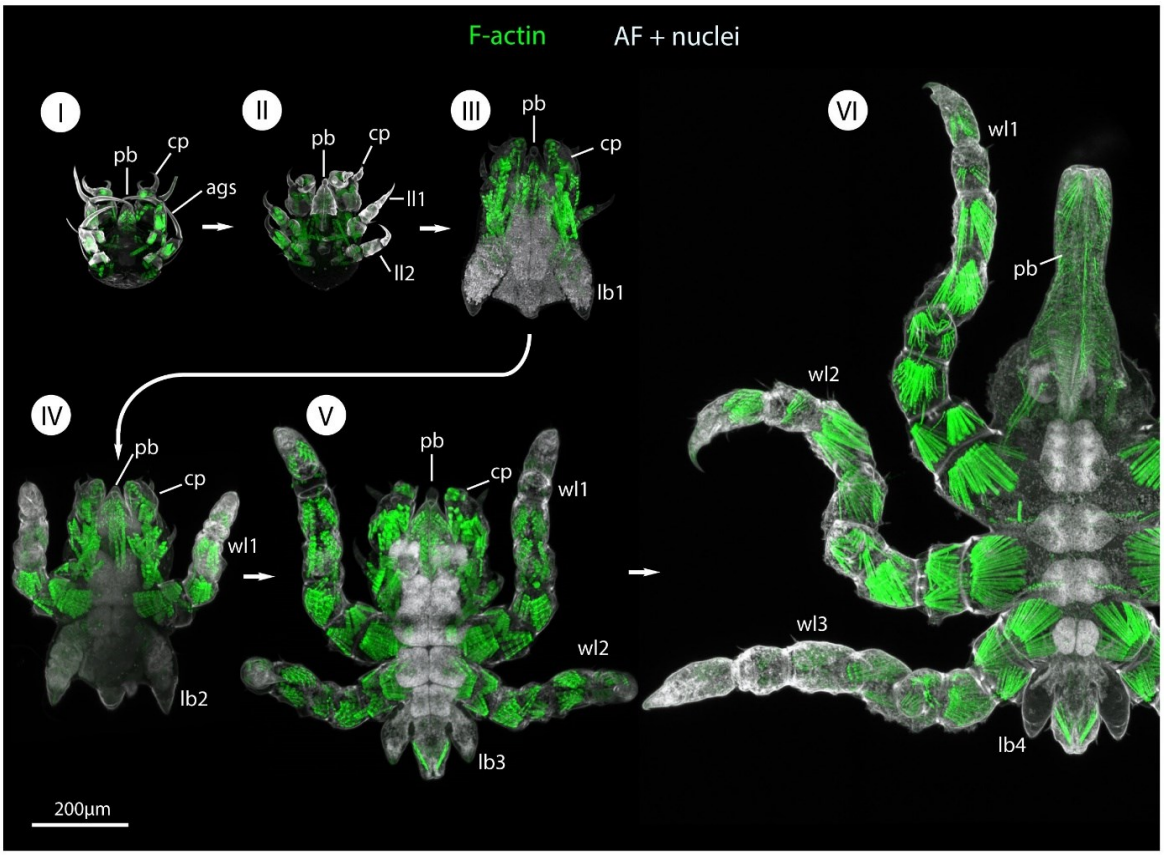

Figure 1: Development of the leg-bearing trunk segments in *P. litorale*.
Ventral overviews of instars I to VI (up to scale). Volume renderings (MIP of CLSM scans) showing F-actin (green) and nuclear labelling (grey) coupled with cuticular autofluorescence (grey). Note the successive emergence of the limb buds and articulated walking legs from instars III to VI. Concurrent with its host switch, instar VI has lost the cheliphores and larval legs and the proboscis is significantly enlarged and remodelled.

AF, autofluorescence; ags, attachment gland spine; cp, cheliphore; pb, proboscis; lb1-4, limb bud 1-4; ll1-2, larval leg 1-2; wl1-3, walking leg 1-3.

The newly acquired tarsus is a so-called pseudopodomere that does not possess its own musculature (Dencker 1974), but rather provides additional movement capabilities between the tibia and the propodus. In contrast to the first leg, the previously seven-articled second leg attains both novel podomeres simultaneously, while the third leg emerges from the limb bud already fully developed with all nine podomeres at instar VI (Vilpoux and Waloszek 2003; Alexeeva and Tamberg 2021; Behrens 1984). With instar VI the anamorphic developmental period of *P. litorale* comes to an end, as all trunk segments and walking leg anlagen are developed (even if not yet fully differentiated).

With every molt from instar II to VI also a new body segment emerges in *P. litorale*. These body segments bear dorsal and ventral sets of longitudinal trunk musculature in adult pycnogonids (Dencker 1974). Brenneis et al. (2023) depicts an instar IV and V of *P. litorale* bearing the first set of longitudinal trunk musculature, hinting at separate development points of trunk segments and its musculature. At the posterior end of the body, the formation of the anal tubercle occurs during the anamorphic development phase. Within the anal tubercle, the ectodermal hindgut is located between the midgut to the anus (Fahrenbach and Arango 2007). The slit-shaped anus, located at the distal end of the anal tubercle, becomes first recognizable at instar V, being fully functional and open at instar VI (Vilpoux and Waloszek 2003; Alexeeva and Tamberg 2021).

At the end of the anamorphic developmental phase of *P. litorale*, an obligatory host switch occurs. While the five first instars feed on the colony-forming hydrozoan *Clava multicornis* (Forsskål, 1775), instar VI begins to feed on sea anemones, such as *Metridium senile* (Linnaeus, 1761) (Schmidt and Bückmann 1971; Tomaschko et al. 1997).

Like all pycnogonids, *P. litorale* uses its anterior located proboscis as feeding apparatus. Inside the proboscis, the pharynx and its associated musculature interact in a manner that functions as a suction pump (Fry 1965; Wagner et al. 2017; Fahrenbach and Arango 2007). The pharynx consists of three circular arranged projecting longitudinal radii along the proximodistal axis of the proboscis, which subdivide it into three circular arranged, interradial running antimeres. This configuration leads to a Y-shape of the constricted and a nearly triangular shape of the dilated pharynx in a cross section of the proboscis (Fry 1965; Wagner et al. 2017; Fahrenbach and Arango 2007). In the initial five instars, the distal tip of the proboscis features a circular mouth opening with a sharp edge that is inserted into the stolons of the hydrozoan host for feeding (Vilpoux and Waloszek 2003; Alexeeva and Tamberg 2021; Behrens 1984; Schmidt and Bückmann 1971).

After the molt to instar VI, the proboscis emerges substantially longer and broader than before, ending in three newly formed triangular symmetrical jaws distally situated in an “Y”-like pattern. This pattern reflects the internal triradiate symmetry of the pharynx and its muscles (Alexeeva and Tamberg 2021; Vilpoux and Waloszek 2003; Fahrenbach and Arango 2007; Wagner et al. 2017). To date, descriptions of the pycnogonid proboscis musculature are restricted to the protonymphon larva of two pycnogonid species (Meisenheimer 1902; Alexeeva et al. 2017) and to the much more complex proboscis musculature of adult pycnogonids (Dencker 1974; Fahrenbach and Arango 2007; Wagner et al. 2017). Comparison between both ontogenetic stages demonstrates that the proboscis musculature has to undergo significant changes and elaboration during the anamorphic development phase. A detailed description of these myoanatomical changes during proboscis growth and reconfiguration is currently lacking for any pycnogonid species.

Thesis aim and research questions

Given the current state of knowledge on the skeletomusculature in the protonymphon larva of two pycnogonid species compared to adults of various other species, it can be inferred that significant new formation and remodelling of the skeleto-musculature occurs during the anamorphic developmental phase of pycnogonids. However, the exact location, sequence and timing of muscle development is still unknown. The overarching aim of this thesis is therefore to provide a detailed description of the development of the skeletomuscular system during the anamorphic developmental phase of *P. litorale.* As outlined above, trunk segments, limb buds, walking legs and the anus are formed during this period. In addition, the proboscis undergoes change and grows in size with the host shift at instar VI. Accordingly, especially these suspected “hot-spots” of muscle development were subjected to close examination to create a data foundation to answer questions about *P. litorales* and pycnogonid myogenesis in general. To some of these muscle development hot-spots, additional research questions were assigned.

1) Regarding the leg muscle development within the limb buds, the main question is, whether the leg muscles develop successively from the proximal to the distal podomeres, according to the proposed ancestral mode of leg muscle myogenesis in crustaceans (Harzsch and Kreissl 2010). Additionally, it will be inquired how the differentiating walking legs are folded within the pre-molt limb buds and if there are any differences in terms of muscle development between the first three walking leg pairs.

2) Based on the comparison of the complex proboscis muscle systems of adult pycnogonids and the modest proboscis muscle systems of protonymphon larvae, the proboscis of *P. litorale* is

predicted to undergo considerable muscle remodelling during its ontogeny. Given the similar external proboscis shape of all postlarval instars feeding on *C. multicornis*, it is hypothesized that the proboscis myoanatomy likely undergoes the most significant changes during the instar V, which precedes the host shift of instar VI with its enlarged proboscis (Fig. 1). To test this, the proboscis musculature will be studied and reconstructed over the complete series of postlarval instars.

3) Finally, the investigation of the myogenetic hot-spots and their developmental patterns promises to provide first insight into the cells underlying myogenesis in *P. litorale*. This will represent the first cell-level data for Chelicerata, affording the opportunity to elucidate if there are similar processes at work during the myogenesis of Pycnogonida as in insects and crustaceans. In particular, if mononucleated pioneer cells (founder cells) fuse with myoblasts to form multinucleated (syncytial) muscle precursor cells, which then fuse with additional myoblasts to form syncytial muscle fibers (Baylies, Bate, and Gomez 1998; Schröter et al. 2004) in *P. litorale*. If so, this might indicate that a founder cell-based mode of myogenesis may represent an evolutionarily conserved feature of all arthropods.

Materials and Methods

Animal Cultivation

The developmental instars of *P. litorale* were obtained from a laboratory culture at the Biology Building of the University of Vienna. The first specimens for this cultivation were collected in the rocky intertidal of the German offshore island Helgoland in the North Sea and near Trondheim in Norway.

In several artificial sea water (ASW) aquaria (ca. 32‰ salinity, 15 to 16 °C), adults and juveniles were kept separately in small groups in net cages (16.5 × 12.5 × 13 cm) together with their feeding host, the sea anemone *Metridium senile* (see Brenneis et al. 2023*)*. In these breeding cages, adult males and females were kept together and checked regularly for males carrying egg batches.

Egg batches were separated from the male's ovigers with soft forceps and subsequently placed into sealable plastic containers supplied with oxygen for the duration of embryonic development.

Once the protonymphon larvae of *P. litorale* started hatching, small pieces of the egg batches were transferred on plastic plates overgrown with the hydrozoan *Clava multicornis*, the feeding host for the initial five postembryonic instars. Plastic plates were infested with larvae at different time points. Given the extended postembryonic development period of *P. litorale*, up to three plastic plates were infested in parallel to facilitate convenient access to the diverse developmental stages essential for the study. The plates were stored on plastic scaffolds within one of the sea water aquaria.

Staining reagents, buffers and solutions used during experimentation

A comprehensive list of buffers and solutions and their ingredients used in the experiments is given in Appendix 1. Details on the staining reagents and mounting media used for fluorescent histochemistry, immunohistochemistry (IHC) and hybridization chain reaction RNA-fluorescent in-situ hybridization (HCR-FISH) are given in Appendix 2. An overview of all staining experiments is provided in Appendix 3. The sequences of the used probe pairs during HCR-FISH can be found in Appendix 4.

Specimen fixation and storage

Post-larval instars I to V and the first juvenile instar VI of *P. litorale* (see Vilpoux and Waloszek 2003) were identified and manually collected from the plastic plates under a stereomicroscope. To relax the muscles and counteract cramping during fixation, the animals were placed in carbonated filtered-artificial-seawater (FASW) for up to 10 minutes. Afterwards they were fixed in 4% paraformaldehyde in FASW (PFA/FASW; 20% methanol-free formaldehyde diluted 1:5 in filtered-artificial-seawater) for one, one and a half, or two hours at room temperature. Subsequently, the fixative solution was removed by washing of the specimens in FASW (2x 5 min). The specimens were then subjected to a series of increasing concentrations of phosphate-buffered saline (PBS; App. 1), before being kept in 100% PBS for 30min.

Two approaches were used for the long-term storage of the material. Specimens were placed in PBS containing 0.1% sodium azide (NaN_3) and stored at 4°C, if they were to be used for fluorescent histochemistry and immunohistochemistry. Specimens intended for HCR-FISH (see below) were gradually transferred into absolute methanol (25%, 50%, 75%, 100%) and stored at -20°C.

Pretreatments and specimen dissection

The long-term storage solutions were removed by washing of the specimens in PBS (3x 10 min). To increase the permeability of the cuticle for subsequent staining procedures, they were put in small glass screw-top vials filled with PBS and exposed to 1-10 sonic pulses in a sonication bath (Globaltronics Gmbh & Co. KG; GT-7810A). After a few pulses, the specimens were examined under a stereomicroscope to check for the presence of any cracks in the cuticle, missing setae or limbs. If specimens showed none of these signs of increased permeability they were subjected to additional sonic pulses.

An alternative approach employed as stand-alone or in conjunction with sonication was the dissection of animals. Instars III to VI were dissected in silicone-covered plastic dishes under a stereomicroscope, using micro-scissors. Eyelashes and needles attached to glass pipettes were used for specimen orientation and manipulation.
In addition to cuts either through the transverse or sagittal plane of the animal´s bodies, the most distal end of the claws was removed. Alternatively, the trunk of some specimens was left intact, while part of the walking legs or the cheliphores were amputated.

Following sonication and/or dissection, the specimens were placed in PBTx (App. 1) for one hour at room temperature to further permeabilize the tissue itself.

Fluorescent histochemistry and immunohistochemistry (IHC)

To study the developing musculature and to detect its preceding pioneer and precursor cells in *P. litorale*, histochemical and IHC stainings were performed. To visualize advanced myofibers and fully differentiated musculature, fluorophore-conjugated phalloidin has previously proved a reliable marker in *P. litorale* (Brenneis et al. 2023), as it stains actin filaments in the cortical cytoskeleton as well as in the sarcomeres of the muscle tissue. A stock solution of Alexa Fluor™ 488 Phalloidin (App. 2) was diluted 1:50 in PBTx and the specimens were incubated over two nights in alteration at 4°C and at room temperature on a shaker. The staining quality was then checked under an epifluorescence stereomicroscope (Nikon SMZ25) and if necessary the incubation was extended for another night.

DAPI (App. 2), a histochemical fluorescence stain which binds to adenine-thymine-rich regions in DNA, was used to label cell nuclei. The DAPI stock solution, was diluted 1:1000 with either PBTx or the Alexa Fluor™ 488 Phalloidin PBTx solution. The samples were incubated for at least one hour.

To selectively label early muscle pioneer cells, two antibodies against myosin heavy chains (MHCs) were tested on *P. litorale* for the first time. The monoclonal mouse antibody 016c6 (App. 2) was raised against locust myosin and has been previously demonstrated to cross-react with crustacean muscle tissue but also with muscle pioneer and precursor cells (Kreissl, Uber, and Harzsch 2008; Harzsch and Kreissl 2010; Jirikowski et al. 2010; Jirikowski, Richter, and Wolff 2013). In addition, the MHC monoclonal mouse antibody 017c5 (App. 2) was tested. Likewise raised against locust myosin, it has shown a high affinity for arthropod and vertebrate MHCs in previous studies and has also been used as a marker for muscle pioneer and precursor cells that already contain myosin heavy chains (Jirikowski et al. 2010).

For IHC, pretreated samples were blocked in PBTx + 5% normal goat serum (NGS) (App.1) to minimize non-specific antibody binding (2x 30 min). The stock solution of the primary antibodies 016c6 or 017c5 were diluted 1:10 with PBTx before the samples were incubated for two nights in alteration at 4°C in a refrigerator and at room temperature on a shaker. Samples were then washed in several changes of PBTx (2x 5 min and 4x 30 min) before being placed in

PBTx + 5% NGS for blocking (2x 30 min). The stock solution of Alexa Fluor™ 568 goat-anti-mouse secondary antibody (App. 2) was diluted 1:400 with PBTx. The secondary antibody solution was then filtered through a syringe filter disc (pore size 0,22µm) to remove unwanted contaminants. Samples were incubated for at least one night before the quality of the staining was checked under an epifluorescence stereomicroscope. If necessary, the incubation was prolonged for up to two additional nights, followed by washing in PBTx (3x 30 min).
In the majority of the IHC experiments, DAPI and phalloidin staining was performed simultaneously (App. 3). One experiment was conducted to check whether the secondary antibody binds at any other location in the specimen tissue other than the targeted primary antibody. This was achieved by implementing a control batch in which the primary antibody was not utilized.

After final washing in PBS (2x 30 min), the specimens were transferred into a series of gradually ascending concentrations of Vectashield™ (App. 2) until they were placed in pure Vectashield™ for long-term storage in a refrigerator.

Hybridization chain reaction RNA-fluorescent in-situ hybridization (HCR-FISH)

As the two cross-reactive MHC antibodies were not specifically raised against pycnogonid MHC, the results obtained in the IHC experiments were compared to species-specific gene expression patterns of MHC. To this end, HCR-FISH was performed (Choi et al. 2018; Schwarzkopf et al. 2021; Bruce et al. 2021) using a protocol adapted by. Dr. Georg Brenneis for *P. litorale* instars. Probe sets specific against MHC-striated type 2 (MHCst) had been previously designed based on sequences identified in developmental transcriptomes and a draft genome of *P. litorale*.
Additionally, the expression pattern of the transcription factor myocyte enhancer factor 2 (MEF2) was studied. MEF2 is expressed in a multitude of developing cells in animals, besides in skeletal, vascular, neural, blood and immune system cells, also in muscle pioneer and precursor cells (Pon and Marra 2015). It has been shown to play an important role in the early stages of myogenesis in metazoans (Bour et al. 1995; Subramanian and Nadal-Ginard 1996; Lin et al. 1996; Price and Patel 2008; Soler, Han, and Taylor 2012), promising to be earlier expressed in differentiating myocytes than the other markers used in this study. The probe pair mixtures (DNA oligoPools) for both genes were ordered at Integrated DNA Technologies (IDT) (Apps. 4; 5).

Four different approaches were employed to visualize the expression patterns of the target genes (App. 3, experiment 9). Instars II to V were sorted into four groups. In two groups either MEF2 or MHCst were labelled individually and in the third group combined visualization of both gene expression patterns was achieved. In the fourth group a combination of IHC and HCR-FISH was attempted to check for co-localization of MHC protein and transcripts, but this experimental group did not yield satisfactory results. The IHC signal in the combination attempt was weak and unspecific, which was probably due to a post-fixation step in between IHC and HCR-FISH (following Schwarzkopf et al. 2021). In all combination groups, the fluorophore-conjugated hairpins were selected so that their emission spectra did not interfere with one another, the nuclear labelling (DAPI) or the autofluorescence of the cuticle during scanning.

The entire protocol, which included the incorporation of IHC, was completed in a period of five days. On day 1, samples were prepared for the combination attempt of IHC and HCR-FISH. Specimens were gradually rehydrated from methanol into an ascending concentration of PBST (App. 1) on ice, followed by washing in PBST (1x 10 min; 2x 5 min), sonication and dissection. Subsequently, the samples were transferred into low-binding Eppendorf tubes and permeabilized with a detergent solution (App. 1) for 30 min at room temperature. After washing in PBST (2x 5 min) and blocking in PBST + 5% NGS (2x 30 min), they were then incubated overnight at room temperature on a shaker with the primary 016c6 antibody (016c6 diluted 1:10 in PBST).

On day 2, the samples used for the combination treatment of IHC and HCR-FISH were washed with PBST (2x 5 min; 4x 30 min) before blocking in PBST + 5% NGS (2x 30 min). Subsequently, a hairpin initiator-labelled donkey anti-mouse secondary antibody (App. 2) was diluted to a concentration of 0,5µg/mL with PBST, and the samples were incubated overnight at 4°C.

On day 3, the remaining samples (MHC-ST & MEF2, both individually and multiplexed) were prepared for HCR-FISH. This included rehydration and washing steps in PBST followed by sonication, dissection and the permeabilization of the samples, as was done on day 1. The combination sample group, comprising IHC and HCR-FISH, was then subjected to a brief (30 min) post-fixation with a solution of 4% paraformaldehyde (PFA) and PBS, in accordance with the recommendation in Schwarzkopf et al. (2021). Subsequently, all samples were pre-hybridized for 30 minutes in a 50:50 mixture of 5x SSCT and probe hybridization buffer (App. 1) pre-warmed to 37°C, followed by 30-45 minutes in pure pre-warmed probe hybridization buffer. Probe solutions for the two target genes were prepared by the addition of 1,6 pmol of

each probe stock solution (i.e. 1,6µL of 1µM stock) to 180-190µL of pre-warmed probe hybridization buffer. After removal of the pre-hybridization solution and the addition of the probe solution, samples were incubated for 20 hours at room temperature.

On day 4, the probe solution was removed from the samples and stored for re-use. The samples were washed in Probe Wash Buffer (App. 1) at 37 °C to remove any remaining probe solution (4x 15 min), followed by washing in 5x SSCT at room temperature on a shaker (2x 5-10 min). Subsequently, samples were subjected to a pre-amplification equilibration in a 50:50 solution of 5x SSCT and amplification buffer (App. 1) (30 min), followed by incubation for 30-45 minutes in pure amplification buffer. In order to prepare the hairpin mixtures 2.5 µL of eight different hairpin stock solutions (B2-647; B2-594; B4-546 and B5-647, each with hairpin 1 and 2) (App. 2) were heated to 95 °C for 90 seconds and cooled down in the dark to room temperature. Corresponding hairpin pairs were then diluted in 90 µL of amplification buffer. After removal of the pre-amplification buffer from the samples, the hairpin mixtures were applied and incubated for 20 hours at room temperature and in the dark.

On day 5, the hairpin mixtures were removed and stored for re-use. This was followed by two short (5 min) and two long (30 min) washing steps in 5x SSCT. Nuclear staining (DAPI) was performed in 5x SSCT, and the final washing steps were conducted in 5x SSCT. Samples were then transferred into 50% ultra-pure glycerol in PBS for storage at 4° C prior to imaging.

Mounting of samples

To optimize fluorescence signal documentation, the transparency of sample tissues can be increased by different mounting media. To this end, IHC samples were gradually transferred from Vectashield™ into RapiClear™ (App. 2) and mounted in pure RapiClear™. Due to the negative effect of RapiClear™ on HCR-FISH labelling, gene expression samples were subjected to an increasing concentration series of TDE (2,2'-thiodiethanol) with PBS prior to being mounted in 70% TDE/PBS. All specimens were mounted on microscopic slides beneath a cover slip with plasticine feet using a stereomicroscope and eyelashes attached to micropipette tips for specimen orientation.

Data documentation and visualization

The staining quality of the samples was evaluated during the HC and IHC procedures using a Nikon SMZ25 epifluorescence stereomicroscope. Imaging was conducted with a Leica DMI 6000 CS confocal laser scanning microscope (CLSM) coupled to a Leica TCS SP5 II scan unit and the microscope-software platform Leica LAS AF.

The laser lines employed were selected based on the excitation spectra of the fluorescent markers used (App. 2). The CLSM image stacks were analyzed and visualized using the 3D reconstruction software packages Imaris (x64, v7.3.1.) and Amira (v2020.2). 3D volume renderings were calculated as maximum intensity projections (MIP). Segmentation of structures of interest was conducted manually in Amira utilizing the threshold tool. 3D renderings of segmentations were subjected to the functions “island removal” and “smoothing”. All figures were assembled and labelled using Adobe Illustrator (2021).

Selection of terminology

The terminology of pycnogonid musculature is not completely consistent across the few studies available. In this thesis, the nomenclature applied to the podomeres and muscle groups of the walking legs is a combination of the terminologies used by King (1973), Dencker (1974) and Schram and Hedgpeth (1978). The fifth and sixth podomeres, which are labelled as tibia 1 and tibia 2 by King, are in this work referred to as patella and tibia after Dencker (1974) and Schram and Hedgpeth (1978). This is supported by recent findings on the chelicerate patella, which suggest homology of the pycnogonid tibia 1 with the patella in other chelicerates (Klementz et al. 2024). Following Dencker (1974), leg muscles are named after the podomere they are moving not the podomere they are located in. Likewise, Dencker’s terms levator and depressor are used to differentiate between muscles responsible for lifting/stretching of the leg and those lowering/flexing it (contra extensor and flexor in Schram and Hedgpeth 1978).
Musculature moving the leg forward and backward with respect to the primary body axis, are described as protractor and retractor, respectively (contra to promotor, remotor of Dencker (1974), Schram and Hedgpeth (1978) and adductor, abductor of King (1973)).
Concerning the proboscis musculature, terminology is kept close to that of King (1973) and Fry (1965). This excludes the pharyngeal constrictor and the jaw retractor muscles, called circular muscles and lip muscles, respectively, by King (1973). In these two cases, it was decided that the functionally more meaningful terminology is preferable.

The terminology of developing muscle cells is adopted from studies of insect and crustacean myogenesis (Kreissl, Uber, and Harzsch 2008; Jirikowski et al. 2010; Harzsch and Kreissl 2010; Baylies, Bate, and Gomez 1998). Accordingly, the first mononucleated muscle progenitor cell is called a pioneer or founder cell. With the gain of additional nuclei over myoblast fusion they become muscle precursor cells.

In this thesis the term "muscle" is used to describe differentiated multinucleated muscle fibres that contain sarcomeres with actin and myosin filaments, and therefore exhibit striation, whether individually or in conglomerates. In some cases, multiple muscle fibers can insert into a single tendon, thereby forming a functional muscle. However, the bundles of muscle fibers cannot be classified as muscles in the traditional sense, given that they are not enveloped in connective tissue like in vertebrates (Fahrenbach 1994). Despite this, in previous studies as well as in this one, groups of muscle fibers arranged in close proximity with identical orientation and developmental history will be referred to as muscles. Conglomerates of muscles with similar task and location, for example levator and depressor muscles within one podomeres of the leg, will be referred to as muscle groups or complexes.

Results

Differential staining characteristics of protein labelling and candidate gene expression

To trace the developing muscle tissue throughout the anamorphic development of *P. litorale*, transcript (HCR-FISH) and protein (HC and IHC) labelling techniques were employed (Fig. 2). HCR-FISH of the transcription factor MEF2 provided the earliest indication of developing muscle cells (Figs. 2 A, A´; 3 A´´). Given the expression of MEF2 in a multitude of developing cells (Pon and Marra 2015), the signal is relatively unspecific. However, in early muscle development stages, it does provide a general indication of the location of muscle development. This can be observed, for instance, in the limb buds of middle-aged stages of instar III (Fig. 3B´´) and in the initial formation of longitudinal trunk muscles and intermediate leg muscles in instar IV (Fig. 2A´). As muscle development progresses, the MEF2 signal strengthens in the muscle pioneer cells, as seen within the limb bud of instar III (Fig. 3 B´´, C´´) or the longitudinal or intermediate leg muscles (Fig. 2A´). In contrast, HCR-FISH of MHCst provides a highly specific expression signal in developing and differentiated striated musculature by labelling the myosin filaments within the sarcomeres of the contractile myofibrils (Fig. 2A´´). It was also deployed as a control for the monoclonal MHC antibody 016c6.

In this study, the monoclonal antibody 017c5 did not work satisfactorily in *P. litorale* and gave unspecific and weak signals. Therefore, only the results obtained through the antibody 016c6 are being reported. Compared to MHCst HCR-FISH, MHC immunolabelling with the monoclonal antibody 016c6 showed a slightly deviating pattern, which displayed stronger signal intensity in earlier stages of muscle development than in fully differentiated striated muscle fibers (Fig. 2 B, B´´). Additionally MHCst HCR-FISH showed an overall higher specificity for developing striated musculature then MHC immunolabelling (Fig. 2 A´´, B´´), which displayed some seemingly non-specific binding mainly in the area of the digestive tract (Figs. 2B´´; 3B´). Importantly, however, the cell nuclei of pioneer muscle cells were only discernible using the MHC immunolabelling. Owing to this, mononucleate muscle pioneer cells are discernible in MHC-immunolabelled specimens (Figs. 2 B´´; 4 arrows; 5 middle two columns: A´-C´´), enabling detection of muscle pioneer cells prior to their accumulation of F-actin in the myofibrils (Figs. 2 B-B´´; 5 right two columns: A´´-C´´´). This was particularly useful for the uncovering of the sequence of muscle development within the limb bud (Figs. 4; 5). F-actin labelling through phalloidin provides a robust signal in already matured but still developing muscles (Fig. 5C´´´) and fully differentiated musculature (Fig. 2 B, B´).

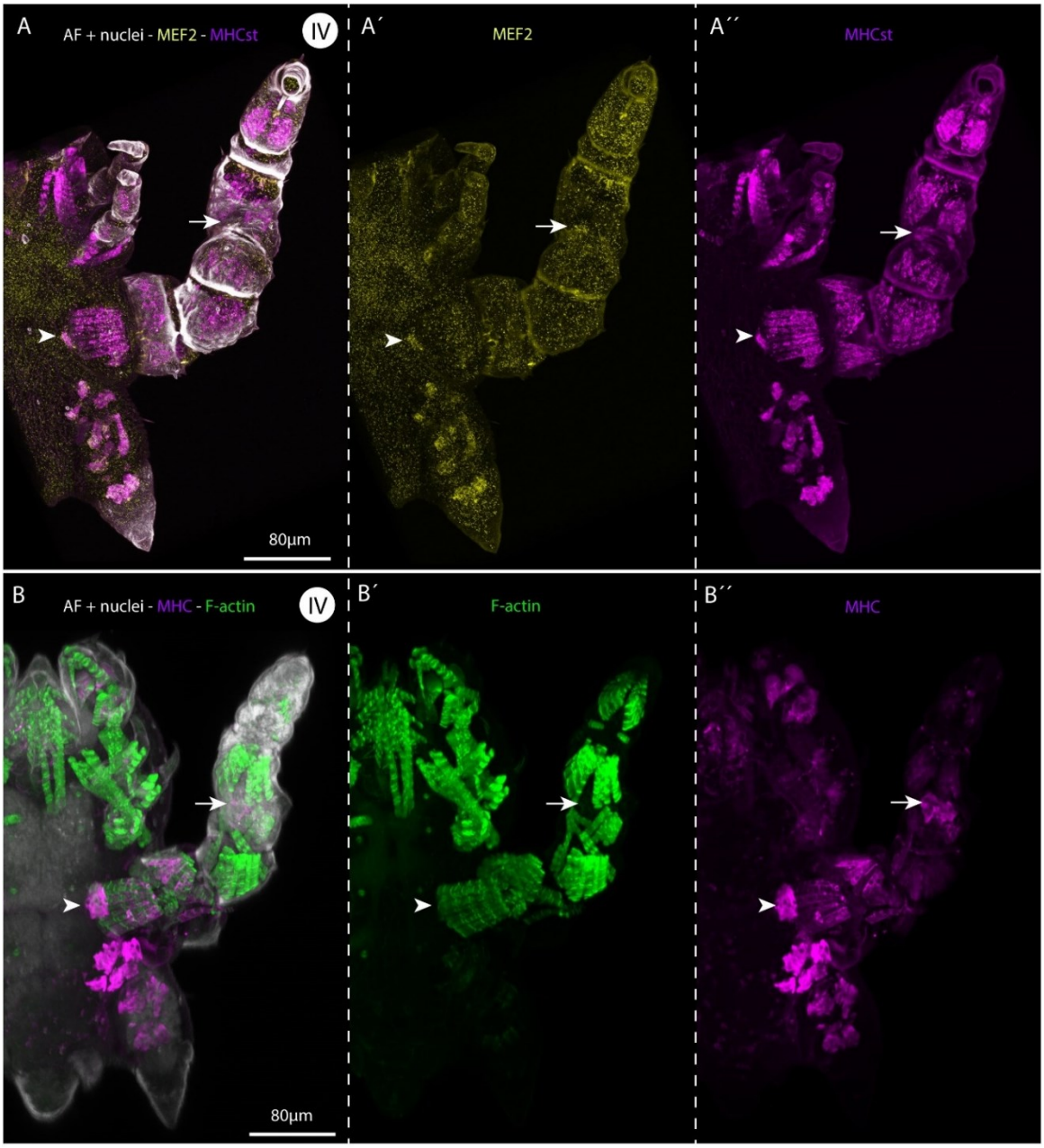

Figure 2: Differential labelling of skeletomusculature and muscle pioneer cells in *P. litorale*. Volume renderings of CLSM scans of two similarly developed instars IV, left body half shown in ventral view. The arrowheads point at developing first ventral longitudinal muscles. The arrows indicate the developing muscles in the future patella. (**A**-**A''**): HCR FISH of myocyte enhancer factor-2 (yellow) and myosin heavy chain striated (magenta) shown in combination (**A**, with cuticular autofluorescence in grey) and separately (**A'**, **A''**). Note the strong MEF2 signal exclusively in early developmental stages of developing muscles in the limb bud, in the patella muscles (arrow) and in the forming longitudinal trunk musculature (arrowhead). By contrast, MHCst is expressed in developing and in fully differentiated muscles (**A´´**). (**B**-**B''**): F-actin labelling (green) and myosin heavy chain immunolabeling (016c6, magenta), shown in combination (**B**, with nuclear counterstain and autofluorescence in grey) and separately (**B'**, **B''**). F-actin labelling is strongest in differentiated muscles, whereas early developmental stages of the longitudinal trunk and patella muscles show only a weak signal. The signal strength after MHC immunolabeling shows a complementary pattern. Note that MHC immunolabeling leads also to some signal in the digestive tract, which is absent in the HCR FISH of MHCst (compare **B''** with **A''**).

AF, autofluorescence; MEF2, myocyte enhancer factor-2; MHCst, myosin heavy chain striated (HCR); MHC, myosin heavy chain (IHC).

Furthermore, in the depiction of F-actin-labelled specimens (Figs. 1; 2B') the striation of the muscle fibers can be easily distinguished, with the bright I-bands, comprising actin filaments associated with z-discs, clearly visible. Next to them the dimmer A-bands are located, with their central situated H-zones, which are comprised of thick hollow-cored myosin filaments with no actin. The Z-discs and therefore the I-bands are located at the borders of the individual sarcomeres comprising the myofibrils. The reconstructions of the proboscis and the walking leg musculature were performed on CLSM scans of F-actin labelled specimens.

Sequence of muscle development and the folding of the leg within the limb bud

The complete musculature of the first walking leg, with the sole exception of the muscles in the future femur, is formed during instar III within the cuticularized limb bud (Figs. 4; 5). In the early stages of instar III, the cell density in the limb buds increases accompanied by the emergence of weak ubiquitous MEF2 expression (Fig. 3 A, A´´). Toward the middle-aged instar III, MEF2 expression is upregulated in the proximal and distal regions of the limb bud (Fig. 3 B, B´´), and first weak expression of MHCst is observed in the region of the extrinsic coxa1 musculature (Fig. 3B´ arrow). The first 016c6 antibody labelling highlights the primordial extrinsic muscles, followed by the muscles in coxa1 and more distally the muscles in the propodus (Figs. 4 A, A´; 5 A-A´´, B-B´´). Only subsequently, the intermediate muscles in coxa2, coxa3, patella and tibia are being formed (Figs. 4 B, B´; 5 C-C´´´). This latter process appears to occur almost simultaneously; a distinct sequence of their formation could not be observed. In particular, the musculature of coxa2, coxa3 and the patella in these early stages is challenging to assign with certainty within the limb bud (Fig. 4 B, B´). The vertical orientation of the coxa2 protractor and retractor muscles however, makes it easy to distinguish them from their distal neighbors during development. The complete absence of propodus levator muscles also facilitates the identification of the propodus depressor muscles in the future tibia during the middle stages of limb bud development (Fig. 4 B, B´). At this stage, the initial folding of the walking leg within the limb bud can be discerned, accompanied by the emergence of podomere borders (Fig. 6 A, B). Before molting, the formation of the podomeres, including cuticle, joints, and musculature, reaches completion (Figs. 3 C-C´´; 4 C, C´; 5 C-D´´´) The muscles consist now of a multitude of mononucleated pioneer cells, giving a strong signal from labelled MHCs as well as labelled F-actin (Fig. 5 C-C´´´). If a singular muscle pioneer cell (a true founder cell) per limb muscle emerges first at the start of muscle formation or a small group of pioneers develop simultaneously could not be definitively determined. The earliest observations of leg muscle pioneer cells were always of small groups, which over the course of development

increased in number (Figs. 4; 5 A-C´´´). In essence, there are two configurations of limb bud between instar III and V. The first and second limb buds, at instar III and IV, respectively, contain seven podomeres with seven muscle complexes prior to molting (Fig. 6 A-C). The third limb bud contains prior to molting a walking leg comprising already all nine podomeres and eight muscle complexes (Fig. 6 D).

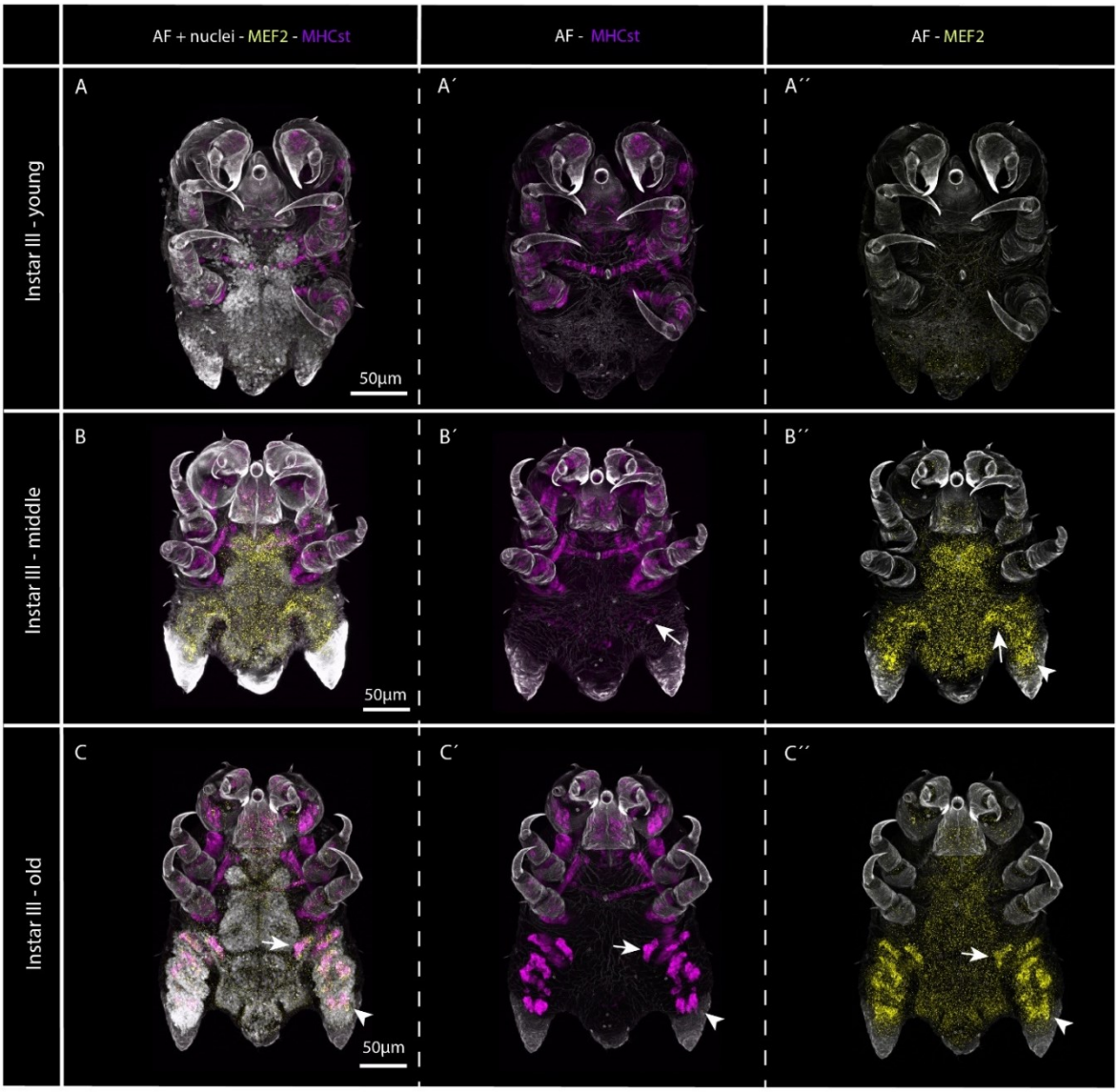

Figure 3: MHCst and MEF2 gene expression in the developing first limb bud of instar III.
Volume renderings (MIP of CLSM scans) of a young, a middle-aged and an old (pre-molt) stage of instar III, shown in ventral view. The arrowheads indicate the developing muscles in the future tarsus-propodus complex (distal leg muscle group). The arrows point at developing extrinsic leg muscles. HCR FISH of myocyte enhancer factor-2 (yellow) and myosin heavy chain striated (magenta) shown in combination (left column: **A-C**, with cuticular autofluorescence and nuclear labelling in grey) and separately (middle and right columns: **A'-C´´**). In the middle-aged stage, the earliest MHCst signal appears proximally in the limb buds, relating to the forming extrinsic leg musculature (arrow in **B´**). In the same stage, strong MEF2 signal is already visible in developing proximal (arrow) and distal leg muscles (arrowhead) (**B´´**). In later stages, MHCst and MEF2 are almost perfectly coexpressed in the developing muscles in limb buds (**C-C´´**).

AF, autofluorescence; MEF2, myocyte enhancer factor-2; MHCst, myosin heavy chain striated (HCR).

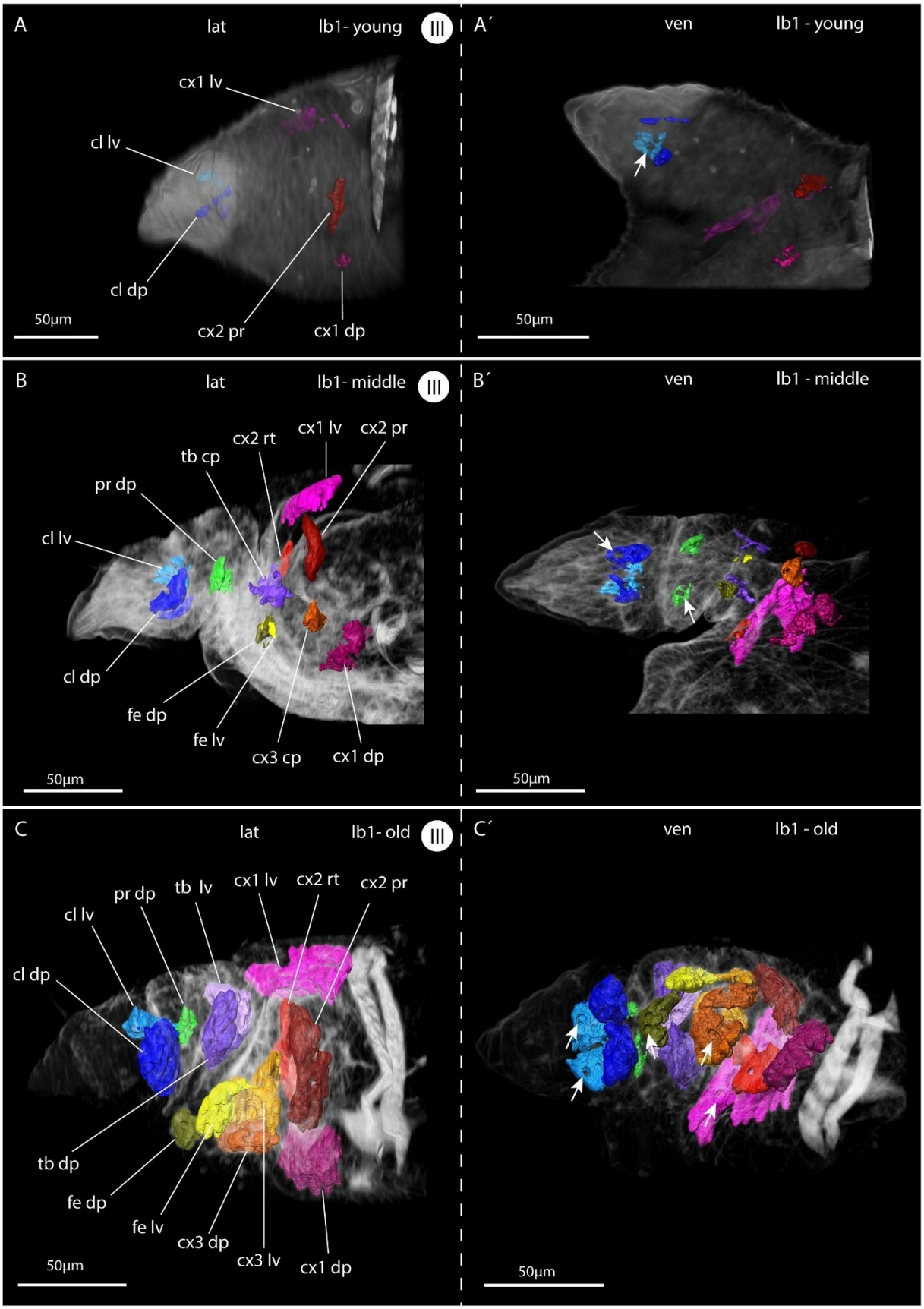

Figure 4: Leg muscle development within the first limb bud of instar III.
The first limb bud of young, middle-aged and old (pre-molt) stages of instar III is shown in lateral (**A, B, C**) and ventral view (**A´, B´, C´**). Reconstructions of the muscles are based on myosin heavy chain immunolabeling (016c6) (with F-actin labelling and cuticular autofluorescence in grey). Arrows point

at nuclei of mononucleated muscle pioneer cells (**A´, B´, C´**). Note proximal (coxa 1 levator and depressor) and distal leg muscles (claw levator and depressor) in the early developmental stage, with first musculature of coxa 1 (coxa 2 protractor) present (**A, A´**)**.** In middle-aged stages intermediate leg muscles have started to form (**B, B´**). Developing muscles are addressed as complexes if a distinction between levator and depressor muscles was not yet possible (**B**). Shortly before the molt to instar IV the completely developed leg muscles are densely packed within the limb bud (**C, C´**)**.**

cl dp, claw depressor; cl lv, claw levator; cx1 dp, coxa 1 depressor; cx1 lv, coxa 1 levator; cx2 pr, coxa 2 protractor; cx2 rt, coxa 2 retractor; cx3 cp, coxa 3 complex; cx3 dp, coxa 3 depressor; cx3 lv, coxa 3 levator; fe dp, femur depressor; fe lv, femur levator; lat, lateral; lb1, first limb bud; pr dp, propodus depressor; tb cp, tibia complex; tb dp, tibia depressor; tb lv, tibia levator; ven, ventral.

The folding of the walking leg within the limb bud cuticle prior to molting remains consistent even with the incorporation of an additional muscle group, exhibiting a Z-shaped folding along the dorso- ventral axis (Fig. 6).

Musculature of the walking legs and their development outside the limb buds

During the molt from instar III to IV, the first walking leg emerges, comprising seven podomeres and seven associated muscle complexes (Fig. 7 A-A´´). The extrinsic musculature is located within the lateral process of the body. It is comprised of two major muscles, the dorsally located coxa1 levator and the ventrally situated coxa1 depressor. They represent the largest walking leg muscles, with the dorsal levator being larger than the ventral depressor (Fig. 7A´´). The muscle group within coxa1 (i.e., coxa2 protractor and retractor) are oriented vertically in a rotated position of 90° in relation to their distal neighbouring muscle groups. The vertically hinged joints between coxa1 and coxa2 enable the walking leg to move forwards and backwards with respect to the body. The coxa2 retractor enables more distal podomeres to move away from the body, with the smaller coxa2 protractor returning them to their original position and even closer to the body. The coxa2-coxa3-joints are rotated horizontally, with the entire podomere of coxa2 exhibiting a slight inward bend (Fig. 7 left and middle column: A-D´). The muscle fibers of the coxa3 levator and depressor are intertwined at the proximal end of coxa2, but from there extend separately in a dorsal or ventral direction, respectively (Fig. 7 right column: A´´-D´´). A unique feature of the coxa3 levator is the extension of some of its muscle bundles through coxa3 to the femur border. By contrast, none of the other leg muscles project across podomere borders. This also applies to most of the muscle fibers of the coxa3 levator with the exception of the most distally located muscle fibers, which stretch into coxa3 to support the femur levator muscles located there (Fig. 7 arrowheads). It is also noteworthy that the supported femur levator, located in coxa3, extends only from anteroventral to anterodorsal

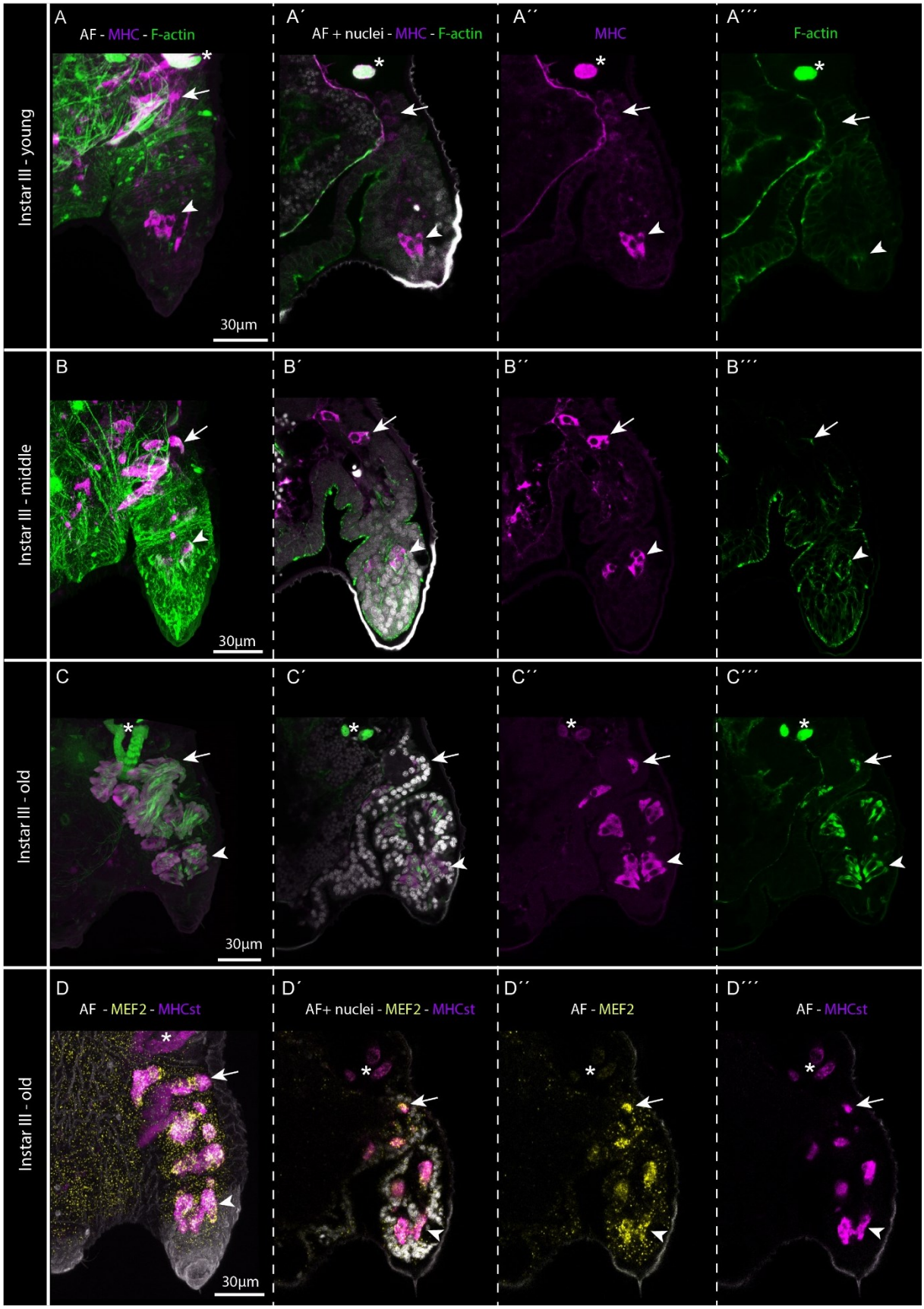

Figure 5: Formation of pioneer muscle cell groups within the first limb bud of instar III.
The first limb bud of young, middle-aged and old (pre-molt) stages of instar III is shown in ventral view, volume renderings (left column: **A-D**; MIP of CLSM scans) and optical sections through the frontal plane (remaining columns: **A´- D´´´**). The arrows indicate the pioneer cells of the developing

extrinsic leg muscles. Arrowheads indicate the pioneer cells of the developing claw musculature. Asterisks mark larval appendage musculature, unrelated to musculature of future walking legs. (**A-C´´´**): F-actin labelling (green) and myosin heavy chain immunolabeling (016c6, magenta), shown in combination (left two columns: **A-C´** with nuclear counterstain and autofluorescence in grey) and separately (right two columns: **A´´-C´´´**). Note the increase in mononucleated muscle pioneer cells of the claw musculature (third column: **A´´ - C´´** arrowhead) and the absence of muscle pioneer cells of the intermediate leg musculature in young and middle-aged limb buds (**A-B´´´**). First strong signal of F-actin in the pre-molt limb bud (**C´´´**)**.** (**D-D´´´**): HCR FISH of myocyte enhancer factor-2 (yellow) and myosin heavy chain striated (magenta) shown in combination (**D, D´** with cuticular autofluorescence in grey) and separately (**D´´, D´´´**). Note the strong MEF2 signal of developing muscles in the limb bud (**D´´**). By contrast, MHCst is more homogeneously expressed (**D´´´**). MHC immunolabeling also leads to some signal in the digestive tract, which is absent in the HCR FISH of MHCst (compare **B''** with **D''**). Note

AF, autofluorescence; MEF2, myocyte enhancer factor-2; MHCst, myosin heavy chain striated (HCR); MHC, myosin heavy chain (IHC).

along the inner/anterior wall of coxa3, showing a clear asymmetry (Fig. 7 arrows), while the outer/posterior wall is supplied exclusively by the elongated coxa3 levator muscle fibers (Fig. 7 arrowheads). In the following distal podomeres, the levator and depressor muscles are each comprised of two identical, along the proximodistal axis of the leg mirrored, muscle bundles, which converge from the lateral walls at the proximal end toward the distal end of the podomere (Fig. 7 middle column: A´-D´). In all podomeres distal to coxa3, the depressor muscles exhibit greater dominance than their antagonists. In the tibia, only a pair of propodus depressor muscles is present, levator muscles are lacking (Fig. 7 right column: A´´-D´´). The musculature within the tarsus-propodus complex (i.e., the claw levator and depressor) enable the movement of the prominent distal claw (Fig. 7 right column: A´´-D´´). After division of the tarsus propodus complex at instar VI the claw levator and depressor stay unaltered in the propodus. Only in advanced stages of instar IV, the femur musculature (i.e., the patella levator and depressor) begins to form, as indicated by first observable MHC immunolabelling (Fig. 2B´´ arrow) as well as HCR-FISH of MEF2 (Fig. 2 A´ arrow) and MHCst (Fig. 2A´´ arrow). In late stages of instar IV, the patella levator and depressor can also be observed with F-actin labelling (Fig. 7 B-B´´) and a new podomere border between the femur and the patella develops. With the molt to instar V, the femur emerges with fully differentiated muscles and fully functional joints (Fig. 7 C-C´´). After the molt to instar VI, tarsus and propodus have separated (Fig. 7 D-D´´). The first walking leg of instar VI is fully articulated and equipped with a complete set of muscles, comprising eight muscle complexes and nine podomeres (Fig. 7 D-D´´). At this stage, the second and third walking legs are also complete, with the emergence of the femur and tarsus of the second walking leg having occurred simultaneously. Also, the third walking leg is already fully articulated with a complete set of muscles, with the patella levator and depressor having developed already in the preceding limb bud stage (Fig. 6 D).

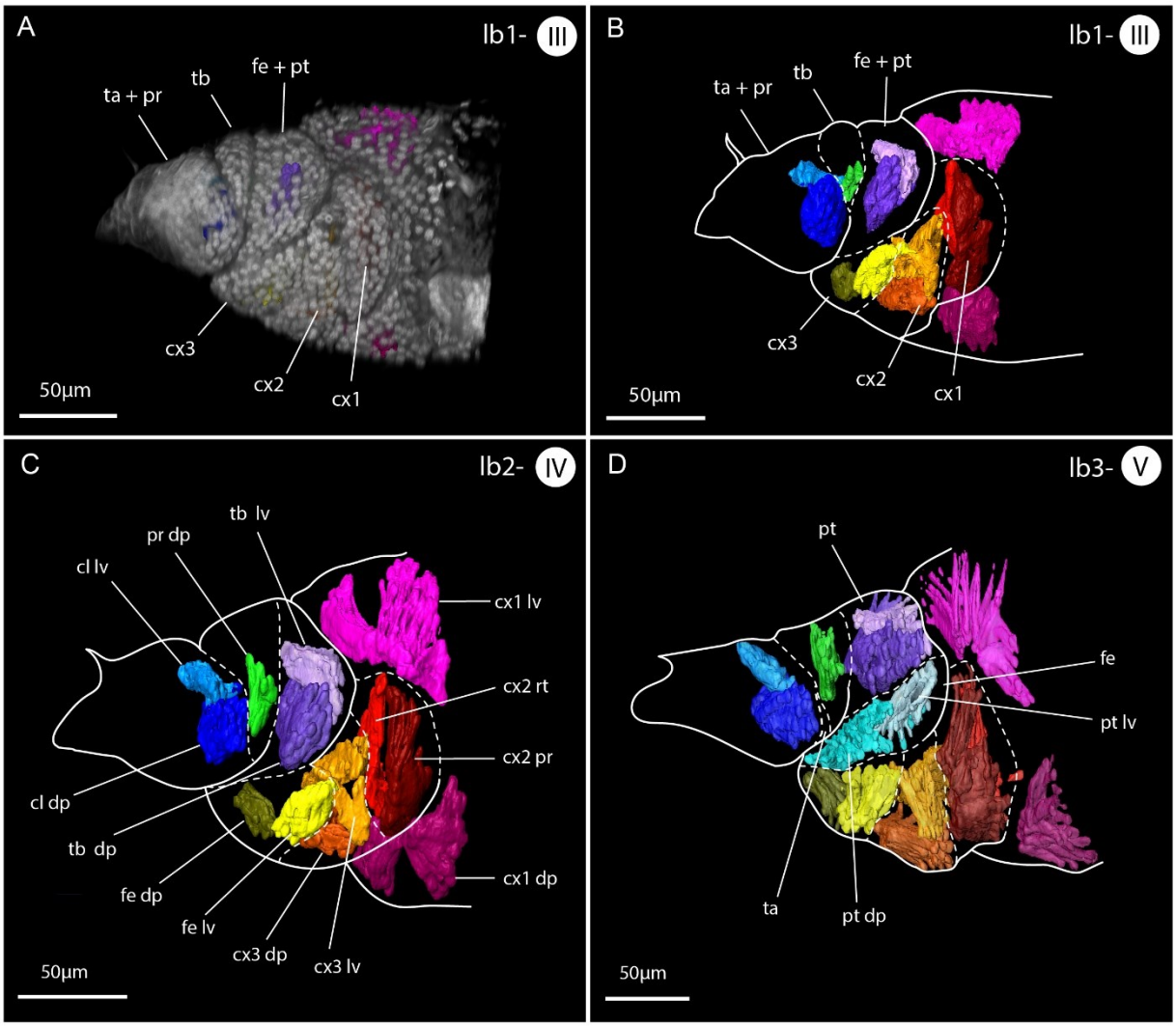

Figure 6: Musculature of the first three legs and their Z-like folding within the cuticularized limb-buds.

Reconstructed musculature of the first three limb buds based on myosin heavy chain immunolabeling (016c6), with schematic drawings of the Z-like folded walking legs inside of the limb buds based on nuclear labelling (**B, C, D**). All limb buds are depicted in lateral view. The continuous drawing line indicates the outline of the walking leg cuticle, while the dashed lines indicate the borders of the podomeres. Labelled podomeres of the first walking leg within the limb-bud of instar III (**A, B**). Nuclear labelling (grey) renders the podomere boarders of the leg visible within the first limb bud, at instar III (**A**). The second limb bud at instar IV with muscles of the second walking leg (**C**). Note that in the first and second limb bud the same muscle groups are present (**B, C**). In comparison the leg within the third limb bud at instar V additionally bears the patella musculature as well as two more podomeres (i.e., femur, patella, tarsus and propodus instead of femur-patella and tarsus-propodus complex) (**D**).

cl dp, claw depressor; cl lv, claw levator; cx1, coxa 1; cx1 dp, coxa 1 depressor; cx1 lv, coxa 1 levator; cx2, coxa 2; cx2 pr, coxa 2 protractor; cx2 rt, coxa 2 retractor; cx3, coxa 3; cx3 dp, coxa 3 depressor; cx3 lv, coxa 3 levator; fe, femur; fe dp, femur depressor; fe lv, femur levator; fe + pt, femur-patella complex; lb1, limb bud of walking leg 1; lb2, limb bud of walking leg 2; lb3, limb bud of walking leg 3; pr, propodus; pr dp, propodus depressor; pt, patella; pt dp, patella depressor; pt lv, patella levator; ta + pr, tarsus-propodus complex; ta, tarsus; tb, tibia; tb dp, tibia depressor; tb lv, tibia levator

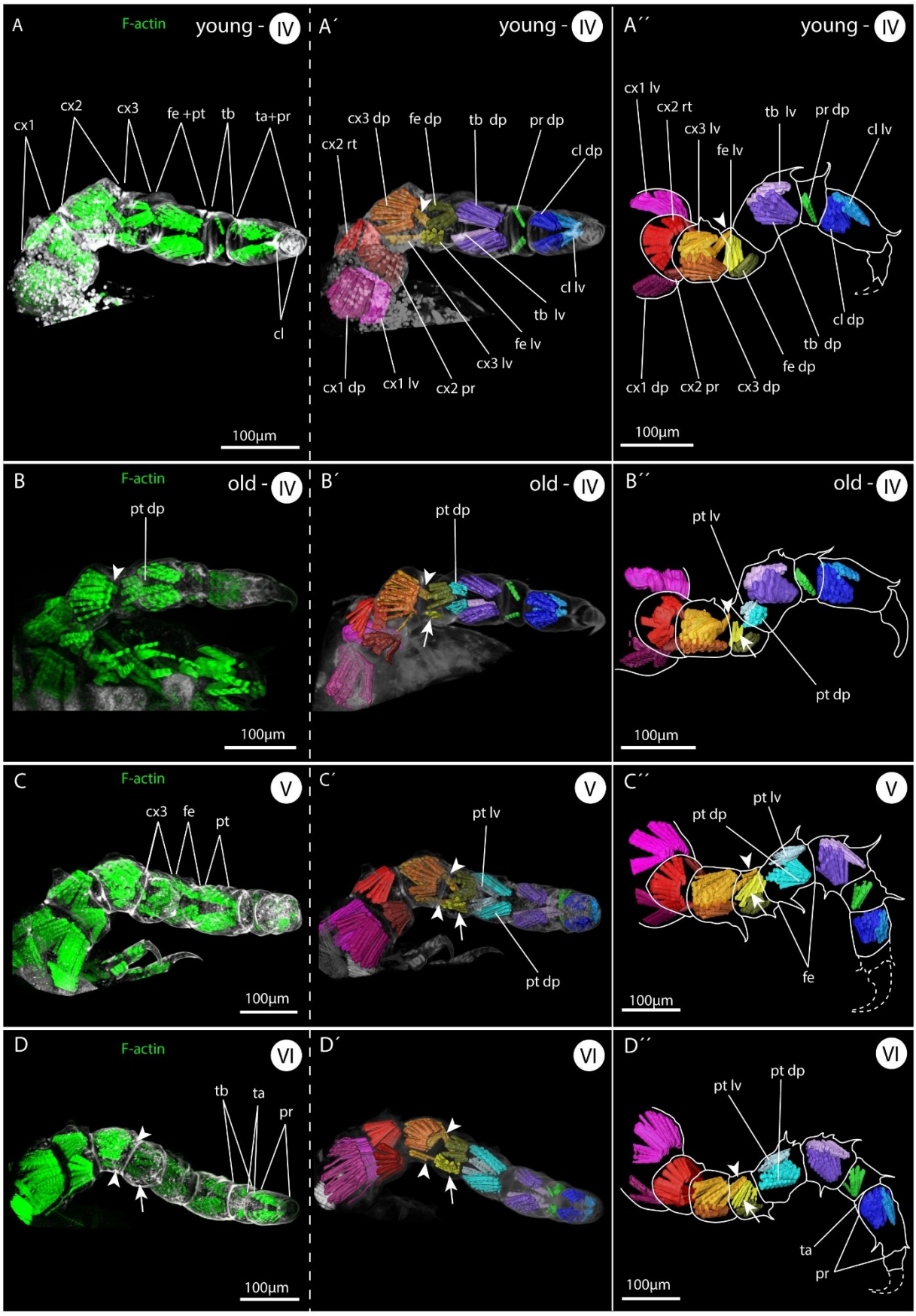

Figure 7: Development of the first walking leg and its musculature throughout instars IV – VI. Volume rendering (MIP of CLSM scans) with F-actin labelling (green) and autofluorescence and nuclear labelling (grey) in ventral view (left and middle column: **A-D´**). Muscle reconstruction (middle and right column: **A´-D´´**) based on F-actin labelling (left column: **A-D**). Volume rendering of the

reconstructed muscle groups with schematic drawings of the podomere cuticle, based on cuticle autofluorescence, in lateral view (right column: **A´´- D´´**). Arrowheads indicate elongated muscle fibers of the coxa 3 levator extending into coxa 3 supporting the femur levator located there. Arrows indicate the asymmetrical femur levator. Note the first walking leg of instar IV is composed of seven podomeres. Formation of the patella musculature in an old instar IV within the femur-patella complex (**B-B´´**). Note that with the molt to instar V, the femur and patella podomeres emerge with the now functioning patella musculature within the newly separated femur (**C-C´´**). With the gain of the non-muscled tarsus, the first walking leg is fully articulated with nine podomeres at instar VI, displaying fully developed and functional muscles (**D-D´´**).

cl, claw; cl dp, claw depressor; cl lv, claw levator; cx1, coxa 1; cx1 dp, coxa 1 depressor; cx1 lv, coxa 1 levator; cx2, coxa 2; cx2 pr, coxa 2 protractor; cx2 rt, coxa 2 retractor; cx3, coxa 3; cx3 dp, coxa 3 depressor; cx3 lv, coxa 3 levator; fe, femur; fe dp, femur depressor; fe lv, femur levator; fe + pt, femur-patella complex; pr, propodus; pr dp, propodus depressor; pt, patella; pt dp, patella depressor; pt lv, patella levator; ta + pr, tarsus-propodus complex; ta, tarsus; tb, tibia; tb dp, tibia depressor; tb lv, tibia levator

Sequence of longitudinal trunk muscle development and description of a new muscle group

The longitudinal trunk musculature is located dorsomedial and ventromedial to the extrinsic coxa1 musculature, in each trunk segment. It mediates movement of the segments to each other. Muscle formation starts in young instar IV with the earliest observations of its development made using MHCst and MEF2 HCR-FISH (Fig. 2 A-A´´). Groups of mononucleated pioneer cells can be distinguished using MHC immunolabelling in instar IV and V (Figs. 2B´´; 8 B, D, E arrowheads). The number of pioneer muscle cells of longitudinal trunk musculature observed was more or less equal to the number of muscle fibers observed of the same muscle in older specimens. In some developing longitudinal trunk muscles fibers, large singular nuclei can still be distinguished through MHC immunolabelling in muscle fibers that have already started to stain for F-actin (Fig. 8 D, D´, E, E´). This contrasts to later, more differentiated muscle fibers, in which such singular nuclei are not recognizable anymore through MHC labelling. In the specimens studied the initial formation of muscle pioneer cells occurred on the ventral side first (Fig. 8B). However, in later stages of some individuals, dorso-longitudinal muscles were observed further developed than their ventral counterparts (Fig. 8 D´, E´).

The first ventro- and dorso-longitudinal pioneer muscle cells of the cephalosoma are formed during instar IV (Fig. 8 A, B) and are fully functional muscles in instar V (Fig. 8 C, D´, E´). During instar V, the pioneer cells of the second ventro- and dorso longitudinal muscles of the cephalosoma begin to appear medial to the first longitudinal muscles (Fig. 8 C-E´). Concurrently, the first longitudinal muscles of the first free trunk segment start to form (Fig. 8 C-E´). As mentioned above, the ventral and dorsal longitudinal musculature may develop slightly asynchronously, and also left and right counterparts do not form in strict synchrony

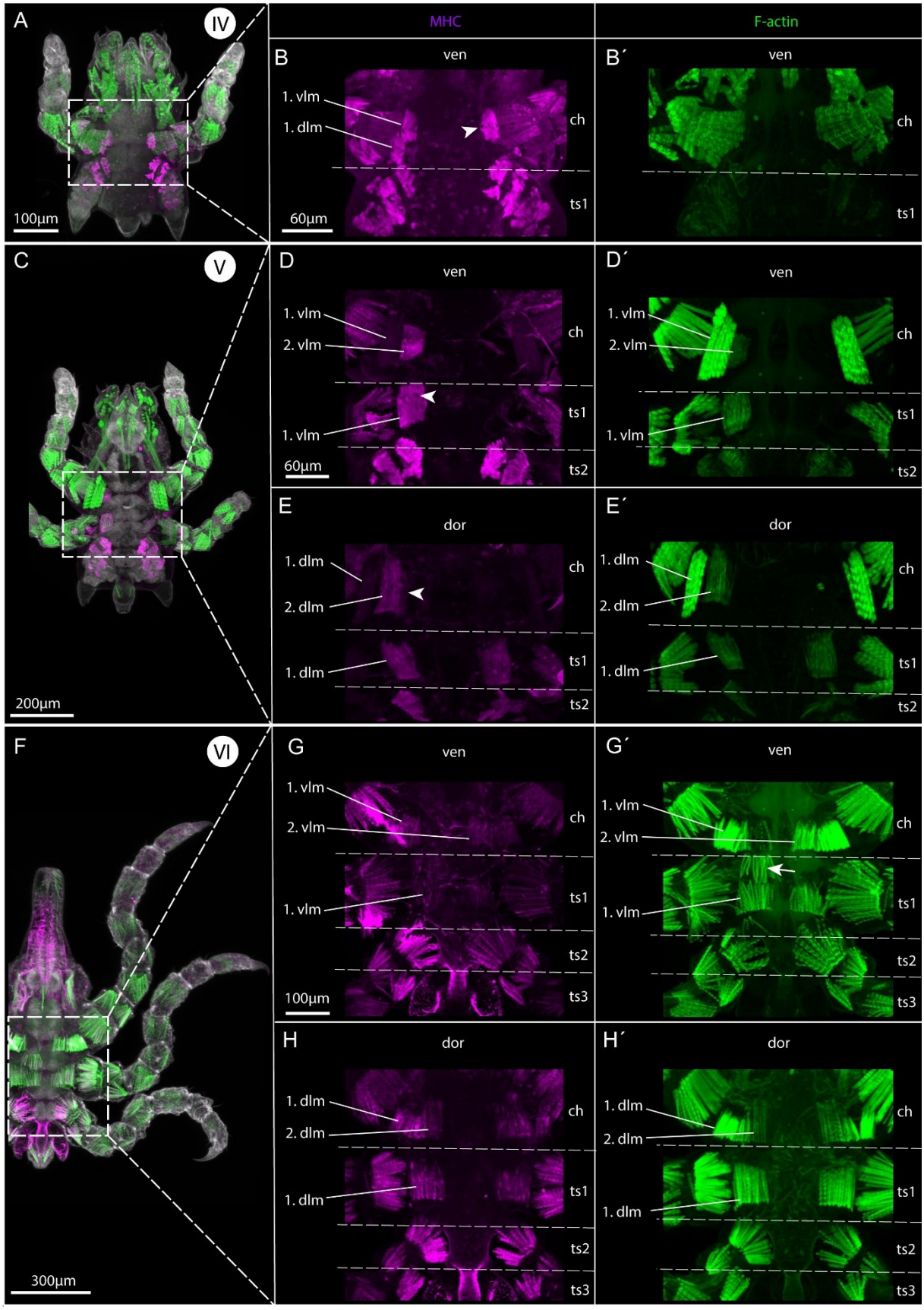

Figure 8: Developmental sequence of the longitudinal trunk musculature throughout instars IV-VI. Volume renderings (MIP of CLSM scans) of the longitudinal trunk musculature of instars iV, V and VI, with F-actin labelling (green), myosin heavy chain immunolabeling (016c6, magenta) and autofluorescence and nuclear labelling (grey). The arrowheads indicate mononucleated muscle

pioneer cells of developing longitudinal musculature. The arrow indicates the by sonication damaged second ventral longitudinal muscle of an instar VI with most of its muscle fibers protruding into the first trunk segment. (left column: **A, C, F**): Overview of instars IV-VI in ventral view, with the dashed rectangle indicating location of detail panels (middle and right column **B-G´**). (**B, B´**): Detail panel of instar IV in ventral view showing MHC immunolabeling (magenta) (**B**) and F-actin labelling (green) (**B´**). Note the strong MHC signal in the first developing longitudinal muscles within the cephalosoma compared to the absent F-actin signal in instar IV (compare **B** to **B´**). (middle and right column **D-H´**): Detail panels are presented in dorsal and ventral views, with the respective opposite body side removed to facilitate visualization of only the dorsal or ventral longitudinal musculature, separately shown with MHC immunolabeling (magenta) (middle column: **B-H**) and F-actin labelling (green) (right column: **B´-H´**). (**D, D´, E, E´**): shows developing longitudinal muscles in instar V. Note the developing second longitudinal musculature of the cephalosoma and their stronger MHC signal compared to the already striated first longitudinal muscles (**D, E**). In comparison F-actin labelling produces a stronger signal in the differentiated first longitudinal muscles of the cephalosoma than in the developing second longitudinal muscles (**D´, E´**). At Instar VI the longitudinal muscles of the cephalosoma and the first trunk segment are fully developed and the signal of the labelled MHC is relatively weak (**G, H**), in comparison labelled F-actin gives a homogenous and strong signal (**G´, H´**).

Ch, cephalosoma; 1. dlm, first dorsal longitudinal muscles; 2. dlm, second dorsal longitudinal muscles; dor, dorsal; MHC, myosin heavy chain (IHC); ts, trunk segment 1; ts2, trunk segment 2; ts3, trunk segment 3; ven, ventral; 1. vlm, first ventral longitudinal muscles; 2. vlm, second ventral longitudinal muscles

with one another, but rather emerge over the course of a single instar stage. At instar VI, the first and second longitudinal musculature of the cephalosoma and the first longitudinal musculature of the first trunk segment are well differentiated and fully functional ventrally (Fig. 8 F, G´, H´) with the dorsal longitudinal muscles being a bit behind in development to their ventral counterparts shown by the stronger signal of labelled MHCs (Fig. 8 G, H). As the oldest stages studied were young and middle-aged instar VI the development of the longitudinal muscles was not followed beyond this state. Accordingly, should secondary longitudinal muscles emerge in any of the free trunk segments, their formation can be inferred to commence in the old stages of instar VI at the earliest.

The development of the anus musculature and its division in two distinct muscle groups

The musculature within the posteriorly located anal tubercle starts to differentiate in young to middle-aged stages of instar IV. The earliest observations of muscle pioneer cells of the future proctodeal dilator musculature were made using MHCst and MEF2 HCR-FISH (Fig. 9 A, B). In middle-aged instar IV, the first expression of MHCs of these muscle pioneer cells can be seen using MHC immunolabelling (Fig. 9C). In older stages of instar IV, F-actin labelling produces a robust signal in differentiated muscle fibers of the anus dilator muscles, stretching from the inner walls of the anal tubercle to the slit-like anus anlage (Fig. 9D arrow). However, additional weaker signal is given by the labelled F-actin of muscle fibers stretching from the

inner walls of the anal tubercle (Fig. 9D arrowhead) to a valve at the border of the mid- and hindgut (Fig. 9D grey arrowhead), indicating an earlier stage of development. Additionally, F-actin labelling reveals the visceral musculature of the midgut (Fig. 9 D-F asterisks). With the molt to instar V, the anlage of the slit-like anus emerges (Fig. 9E grey arrowhead). At this point, both muscle sets, the one connecting to the anus opening (Fig. 9E arrow) and

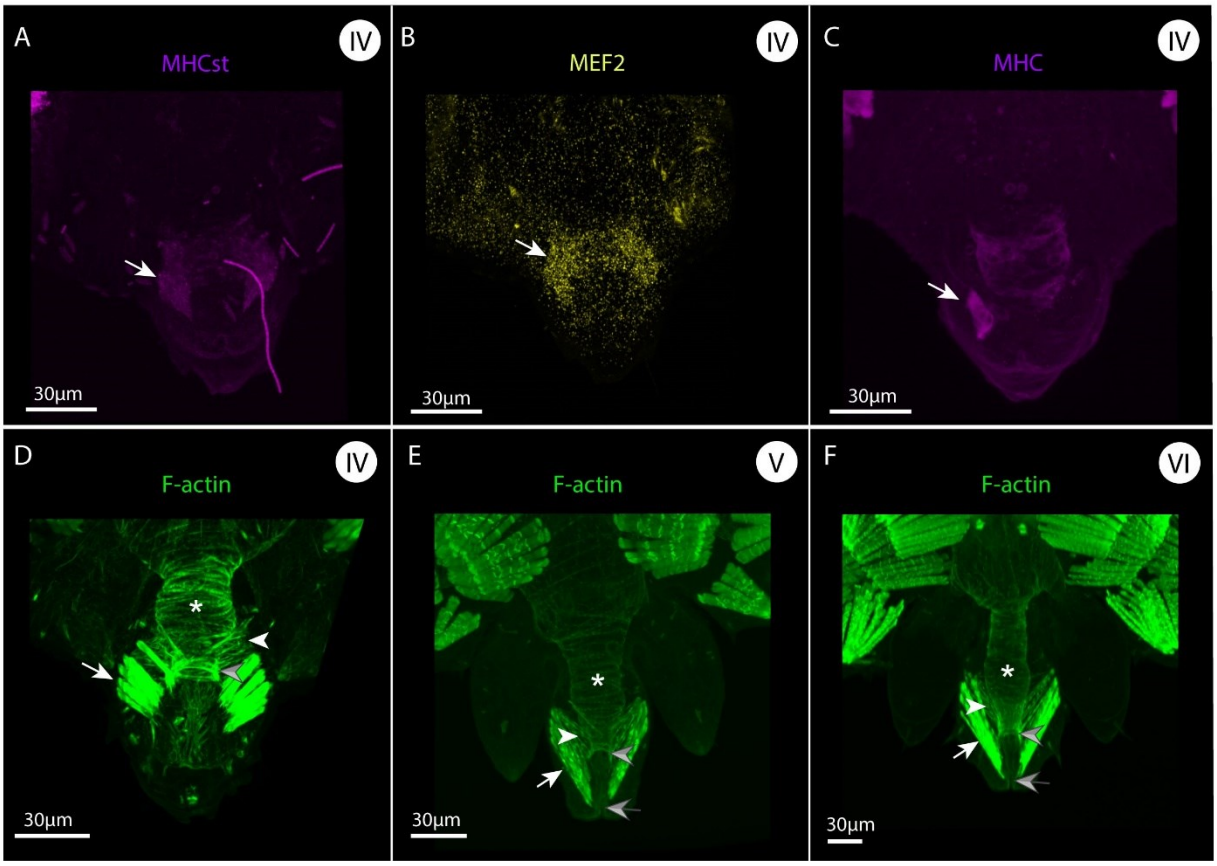

Figure 9: Development of two groups of proctodeal dilator muscles within the anal tubercle throughout instars IV-VI.
Volume renderings (MIP of CLSM scans) of the development of proctodeal dilator musculature in ventral view in instars IV, V and VI. The white arrows indicate developing and differentiated anus dilator musculature. The white arrowheads indicate developing and differentiated dilator musculature of the mid-gut hind-gut boarder valve. The grey arrows indicate the slit-like anus at instar V and VI. The grey arrowheads indicate the mid-gut hind-gut boarder valve. The asterisks mark the visceral musculature of the mid-gut. (**A, B**): HCR FISH of myosin heavy chain striated (magenta) and myocyte enhancer factor-2 (yellow) expression in an instar IV. Note the strong and homogeneous MHCst signal (**A**) and the likewise strong but more heterogeneous MEF2 signal (**B**) in early developmental stages of the developing anus dilator muscles. Myosin heavy chain immunolabeling (magenta) in a middle-aged instar IV, with mononucleated muscle pioneer cells of the anus dilator musculature (**C**). F-actin labelling in an old instar IV (**D**). Note that the anus dilator muscles are further differentiated (white arrow in **D**) then the muscles of the mid-gut hind- gut boarder (**D** white arrowhead). F-actin labelling of instar V and VI showing two groups of differentiated proctodeal dilator muscles (**E, F**). Note the similarity in musculature between instars V and VI even though the anus becomes functional in instar VI (compare **E** with **F**).

MEF2, myocyte enhancer factor-2; MHCst, myosin heavy chain striated (HCR); MHC, myosin heavy chain (IHC)

the other one connecting to the valve at the mid to hindgut border (Fig. 9E arrowhead), seem fully developed. It appears that no additional muscle fibers are formed in the anal tubercle during the transition to instar VI, despite a general increase in size. At instar VI, the anus is now for the first time fully functioning (Fig. 9F).

The development of proboscis musculature from instar II to early stages of instar V

From instar II to early stages of instar V the proboscis muscles can be subdivided into three functional groups, namely the extrinsic proboscis retractor musculature, the dilator muscles of the pharynx and the constrictor musculature of the proximal pharynx (Figs. 10; 11; 12 left column: A-A´´´; 13 left column: A-A´´). The extrinsic proboscis retractor musculature is composed of two large lateral muscle bundles and one dorsal muscle bundle, which extend from the proximal base of the proboscis posteriorly behind the larval legs (Fig. 10 A´´´-C´´´). Consequently, in instars II and III, the muscles pass through the majority of the body (Fig. 10 A´´´, B´´´), reaching the inner side of the dorsolateral body wall anterior to the first limb buds in instar III (Fig. 10 B´´´) and the same region of the cephalosoma anterior to the first walking leg pair in later instars (e.g., Fig. 10 C´´´). These muscles are responsible for the movement and alignment of the proboscis. The lateral extrinsic retractor muscles undergo continuous growth via further addition of muscles fibers and the elongation of these muscles throughout the anamorphic phase of development (Figs. 10 A´´´-C´´´; 11; 12 A´´´-C´´´; 13), reaching its peak in late instar V (Figs. 12 C´´´; 13 C, C´´).

The pharynx dilator musculature can be subdivided into interradial and radial muscles (Fig. 10A´-C´). The interradial dilators are already well-developed in instar II and are arranged in two complexes, one proximal and one distal along the pharynx. Each complex consists of three pairs of muscle fiber rows that attach along the interradial groves in between the pharyngeal radii . Each of the three pairs gradually taper to a point at the inside of the proboscis wall (Fig. 10A´-C´). From instars II to IV, the distal interradial dilator complex retains its original configuration, only slightly increasing in size without the addition of further muscle fibers. This stands in contrast to the proximal interradial dilators, which expand in a posterior direction along the pharynx through the formation of additional muscle fibers (Fig. 11).

In contrast to the interradial pharynx dilators, the radial dilator muscle complex has its point of origin at the tip of the pharyngeal radii and extends from there to the inner side of the proboscis wall.

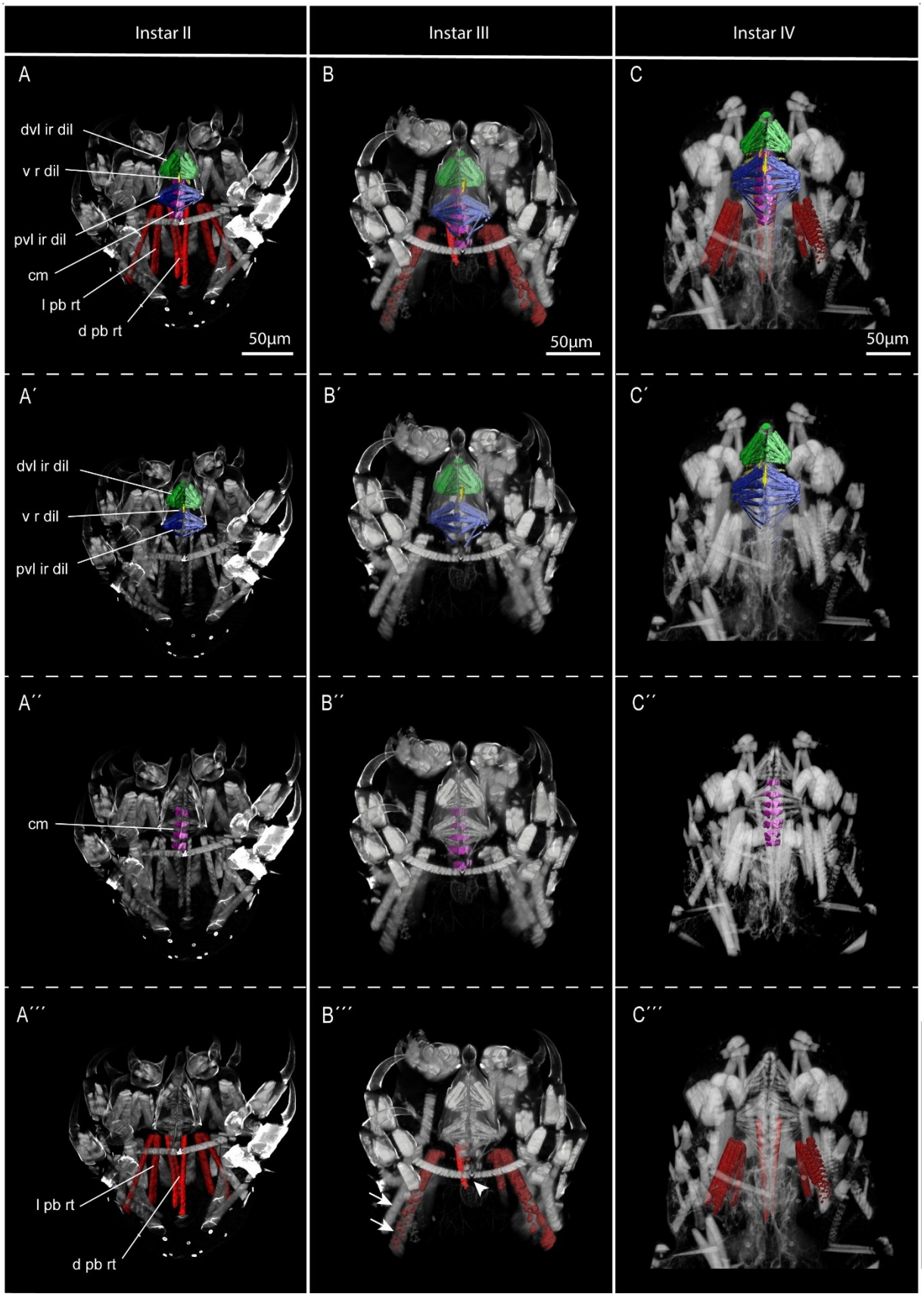

Figure 10: Change of the proboscis musculature throughout instars II-IV.
Volume renderings (MIP of CLSM scans) with reconstructions based on F-actin labelling of the proboscis musculature throughout instars II – IV. With F-actin labelling (grey) and autofluorescence (grey) in ventral view. The arrows indicate insufficient staining of the lateral proboscis retractor muscles. The arrowhead indicates insufficient staining of the dorsal proboscis retractor muscles.

(**A-C**): Overview of instars II, III and IV showing all reconstructed proboscis muscles. (**A´-C´**): Reconstructions of the pharynx dilator muscle groups, distal interradial dilator musculature (green), proximal interradial dilator musculature (blue), radial dilator musculature (yellow). Note the gain of additional muscle fibers of the proximal interradial dilator musculature and the size gain of the radial dilator musculature between instars II and IV. By contrast the distal interradial dilator musculature changes very little. (**A´´-C´´**): Reconstructions of the pharynx constrictor musculature (magenta). Note the gain of additional muscle rings between instars II and IV. (**A´´´-C´´´**): Reconstructions of the proboscis retractor muscles (red). Note the difference in size and the gain of additional muscle fibers of the lateral proboscis retractor muscles between instars II and IV. By contrast the dorsal proboscis retractor muscles undergoes mainly elongation.

cm, constrictor muscles; d pb rt, dorsal proboscis retractor; dvl ir dil, distal interradial dilator; l pb rt, lateral proboscis retractor; pvl ir dil, proximal interradial dilator; v r dil, ventral radial dilator

In instars II to III, the musculature is minute and situated between the proximal and distal interradial dilators on top of the pharyngeal radii (Figs. 10 A´, B´; 11 left and middle column: A-B´´). In instar IV, the radial dilators begin to differentiate further, becoming longer and expanding along the proximo-distal axis of the pharyngeal radii (Figs. 10C´; 11 right column: C-C´´).

The circular constrictor musculature is located in the proximal region of the pharynx (Fig. 10 A´´-C´´). Each muscle ring comprises one dorsal and two ventrolateral muscles (Fig. 11B´), each of which spanning between the tips of the two adjacent pharyngeal radii. The distal-most ring of the constrictor musculature is positioned between the distal and proximal interradial dilator muscle complexes (Fig. 11). Additional rings follow proximally along the pharynx between the insertion sites of the proximal interradial dilator muscle fibers. In instars II to IV, the constrictor muscles function as antagonists to the proximal interradial dilator musculature. Concurrent with the extension of the proximal interradial dilator muscles from instars II to V, also the constrictor muscles form new rings in a proximal direction (Figs. 10 A´´-C´´; 11; 12A´´). Notably, the number of ring muscles does not appear to be stereotypical across different animals within the same developmental stage, as young stages of instar V were observed to have 11 muscle rings (Fig. 12A´´), while some middle-aged instars V featured only 9 muscle rings (Fig. 12B´´).

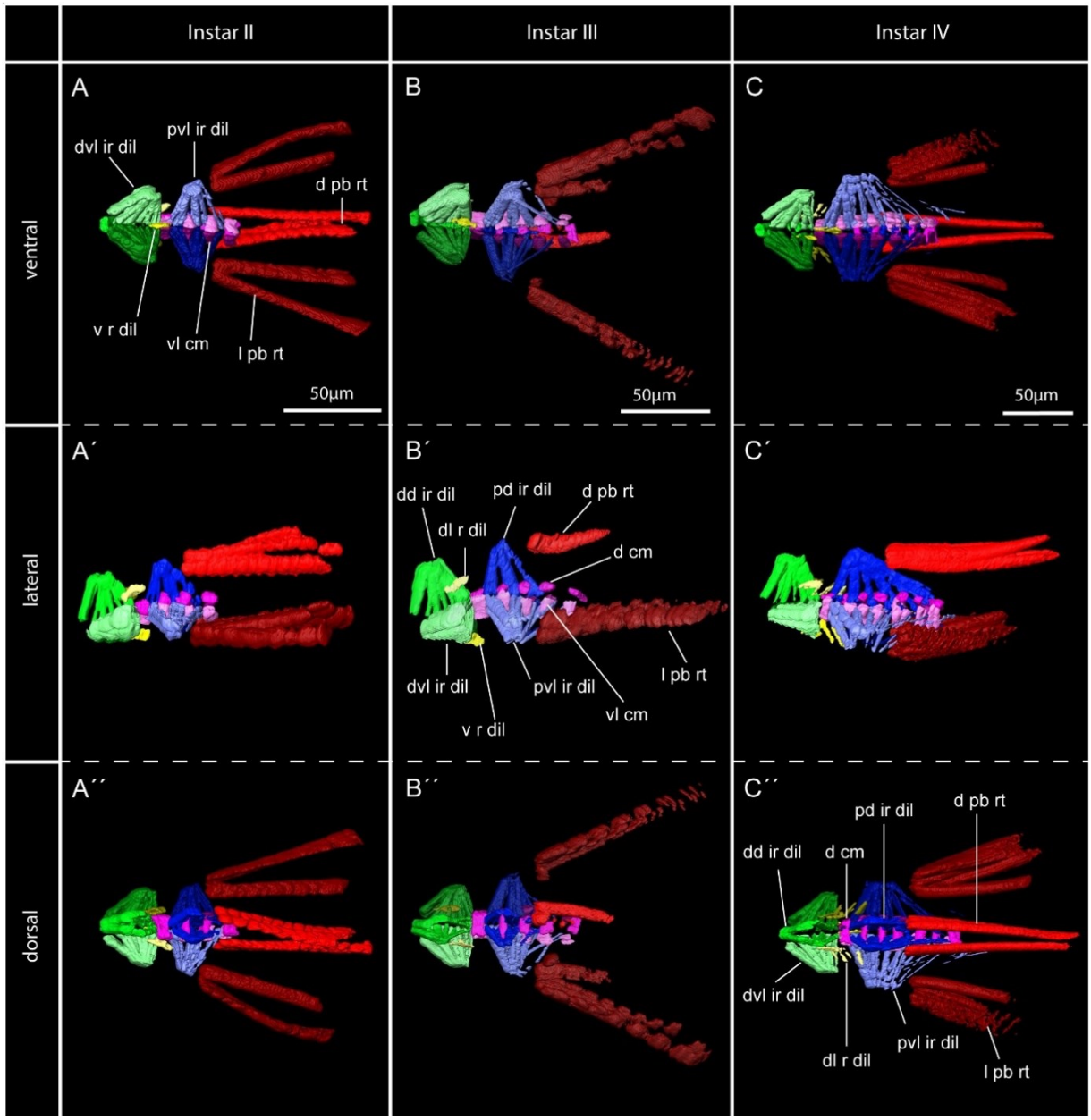

Figure 11: Positioning and configuration of the proboscis musculature of instars II – IV.
Reconstruction of proboscis musculature based on F-actin labelling of instars II-IV in ventral (**A-C**), lateral (**A´-C´**) and dorsal (**A´´ - C´´**) view, showing its triradiate symmetry. Muscle groups are colour coded: distal interradial dilator musculature (green), proximal interradial dilator musculature (blue), radial dilator musculature (yellow), constrictor musculature (magenta), proboscis retractor muscles (red). (left column: **A-A´´**): Instar II with seemingly underdeveloped radial dilator muscles. (middle column: **B-B´´**): Instar III with additional proximal dilator muscle fibers and constrictor muscle rings. (right column: **C-C´´**): interradial and radial dilator muscles with additional muscle fibers and gain of additional constrictor muscle rings. Note that each constrictor muscle rings consists of three muscles (one dorsal, two ventrolateral) and their location between the proximal interradial dilator muscle fibers throughout development. Each of the two interradial dilator complexes consists of three groups of paired fanned out muscle rows. By contrast the radial dilator musculature consists of three groups of single muscle rows. Note the positioning of the radial dilator complex in-between the interradial dilator complexes.

dd ir dil, disto-dorsal interradial dilator; d cm, dorsal constrictor muscles; dl r dil, dorso- lateral radial dilator; d pb rt, dorsal proboscis retractor; dvl ir dil, disto-ventrolateral interradial dilator; l pb rt, lateral proboscis retractor; pd ir dil, proximo-dorsal interradial dilator; pvl ir dil, proximo-ventrolateral interradial dilator; v r dil, ventral radial dilator; vl cm, ventrolateral constrictor muscles

The remodelling of the proboscis and its musculature during instar V

As a consequence of the host shift undergone by *P. litorale* at instar VI, the proboscis undergoes a phase of remodelling during instar V, which significantly impacts the proboscis musculature (Figs. 12 middle and right column: B-C´´´; 13 middle and right column: B-C´´). In early stages of instar V, the proboscis muscles retain a configuration similar to that observed in the preceding developmental stages (Fig. 13 left column: A-A´´). With further development, however, the two interradial dilator complexes spread out along the proximo-distal axis of the pharynx until they are indistinguishable from each other (Fig. 12 B´, C´). Additional muscle fibers are formed in the distal interradial dilator complex, coupled to a reorganization of their attachment sites along the inner side of the proboscis cuticle (Fig. 12B´). Concurrently, the proximal interradial dilator complex undergoes a similar reorganization. This formation of additional, and the prolongation of existing muscle fibers result in a coil-like structure within the proboscis prior to molting (Figs. 12C´; 13 right column C-C´´).

Starting with instar IV, the minute radial dilator experiences substantial growth, reaching a point in late stages of instar V where all three muscle rows extend over the full length of the proboscis along the pharyngeal radii (Figs. 12 B´, C´; 13). Additionally, the densely packed and prolonged muscle fibers coil up in the proximal region of the proboscis shortly before molting, exhibiting a similar pattern of development as the interradial dilators (Fig. 13 C´, C´´). The constrictor muscles are extended posteriorly over the pharynx, with the formation of new muscles occurring during instar V (Figs. 12 A´´-C´´; 13 A´-C´). Additionally, the extrinsic lateral retractor muscles grow via expansion of existing muscle fibers as well as by addition of new ones (Figs. 12 A´´´-C´´´; 13 A-C).

At the distal end of the proboscis, between the reorganizing muscle row pairs of the interradial dilators, the first pioneer muscle cells of the jaw retractors emerge (i.e., in interadial position) in middle-aged instars V (Figs. 12B´´´; 13 middle column: B-B´´). The anlagen of the developing jaw retractor muscles of each interradius are paired (Fig. 12 middle column: B-B''), but transform already during instar V into short and thick muscle rows along the proximo-distal axis at the distal tip of the proboscis (Figs. 12C´´´; 13 right column: C-C´´).

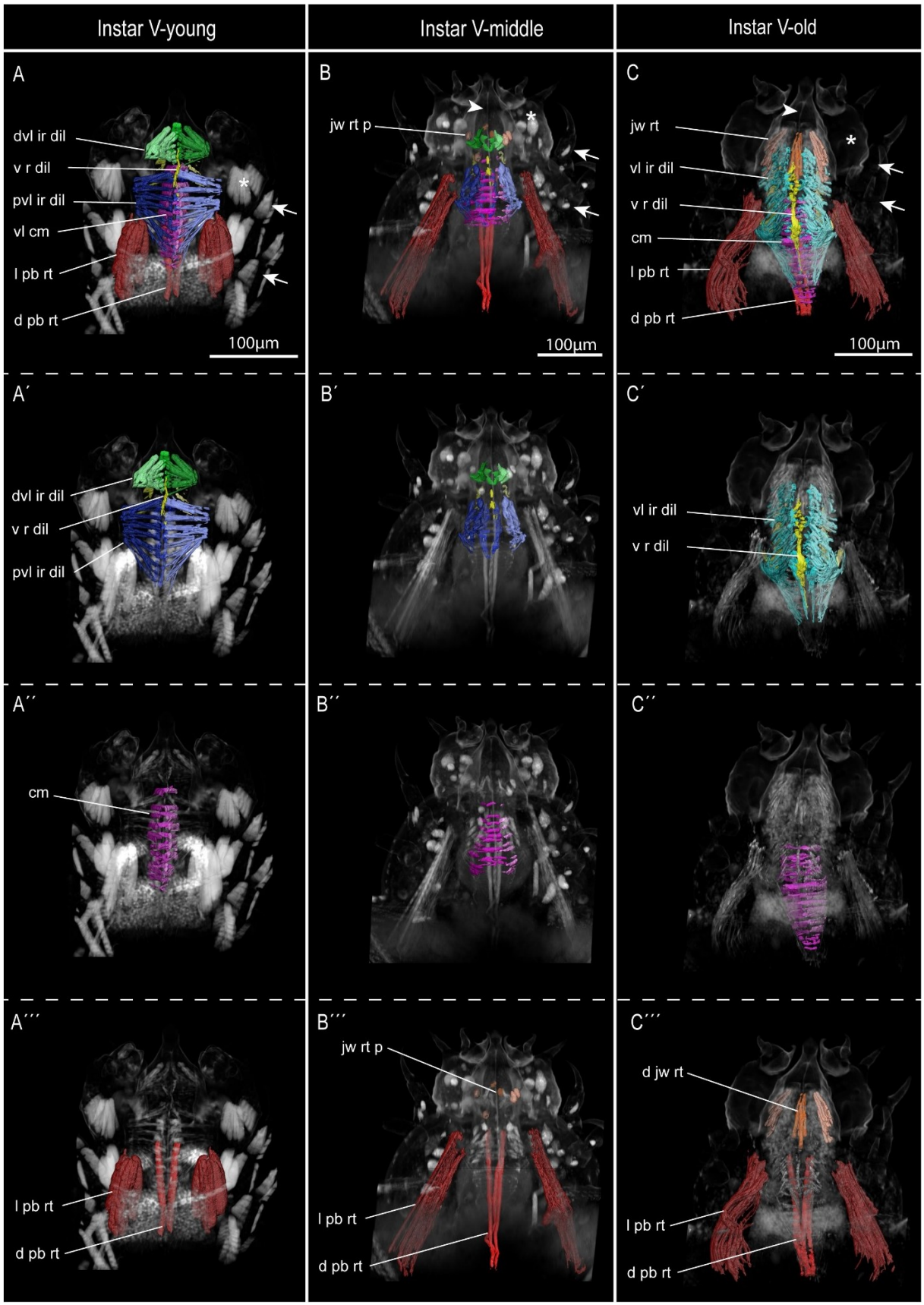

Figure 12: The remodelling of the proboscis musculature of instar V and the emergence of the jaw retractors.

Volume renderings (MIP of CLSM scans) with reconstructions based on F-actin labelling of the proboscis musculature of a young, a middle-aged and an old (pre-moult) stage of instar

V, shown in ventral view. With F-actin labelling (grey) and autofluorescence (grey). The arrows indicate the atrophying larval leg muscles throughout the maturation of instar V (Compare **A - C**). The arrowheads indicate the constricted cuticle husk of the molting pharynx (**B, C**). The asterisk marks the atrophying cheliphore muscles throughout the maturation of instar V (compare **A-C**). (**A-C**): Overview of all reconstructed proboscis muscles. Note that in old instar V the remodelled proboscis musculature is compressed within the old proboscis cuticle (**C**). (**A´-C´**): Reconstructions of the pharynx dilator muscles, distal interradial dilator musculature (green), proximal interradial dilator musculature (blue) and radial dilator musculature (yellow). Configuration of proboscis dilator muscles similar to earlier instars (**A´**). In middle-aged instar V, the dilator musculature partially degenerates (**B´**). Pre-molt, the interradial dilator musculature have merged (light blue) (**C´**). The dilator muscles (radial and interradial) gain additional muscle fibers over the course of maturation of instar V and are pre-molt extended over the full length of the pharynx (**C´**). The proximal dilator muscle fibers coil up inside the new cuticle due to the prolongation of existing muscle bundles (**C´**). (**A´´-C´´**): Reconstructions of the pharynx constrictor musculature (magenta). The pharynx constrictor muscle rings become wider in diameter during remodelling (**B´´**). Note that additional rings appear along the pharynx over the course of maturation (compare **A´´ - C´´**). (**A´´´- C´´´**): Reconstructions of the extrinsic proboscis retractor musculature (red). Note the difference in size and the gain of additional muscle fibers of the lateral proboscis retractor muscles during maturation of instar V, by contrast the dorsal proboscis retractor muscles undergoes mainly elongation (compare **A´´´ - C´´´**). (**B´´´- C´´´**): Reconstructions of the developing three jaw retractor muscles. Note the paired jaw retractor muscle pioneer cells in middle-aged instar V, compared to the distinguished jaw retractors of pre-molt (old) instar V (compare **B´´´** and **C´´´**).

cm, constrictor muscles; d jw rt, dorsal jaw retractor; d pb rt, dorsal proboscis retractor; dvl ir dil, disto-ventrolateral interradial dilator; jw rt, jaw retractor; l pb rt, lateral proboscis retractor; pvl ir dil, proximo-ventrolateral interradial dilator; v r dil, ventral radial dilator; vl cm, ventrolateral constrictor muscles; vl ir dil, ventrolateral interradial dilator.

Prior to the molt to instar VI, the interradial dilator muscle row pairs are separated from each other and are no longer attaching at the same location on the inner proboscis wall. This permits the differentiation of the jaw retractors at the distal end of the proboscis in between the interradial dilator muscle row pairs (Fig. 13 right column: C-C´´). The entire proboscis undergoes a process of compression, during which the recently formed cuticle is folded and tucked into itself (Fig. 14). The folding (Fig. 14 arrowheads) is reflected by the coiling of the proximal radial and interradial pharyngeal dilator muscles (Figs. 12C´; 13 right column: C-C´´)

The remodelled proboscis musculature of instar VI

After the molt to instar VI, the newly emerged proboscis is considerably longer than before (Figs. 15; 16). The interradial dilators are no longer coiled and extend in three interradial double rows (one dorsal, two ventro-lateral) along the entire proboscis (Figs. 15 A, B; 16). Similarly, also the radial dilators are uncoiled and progress as a single row along each pharyngeal radius along the entire length of the proboscis (Figs. 15 A, B; 16). At the distal end of the proboscis, the newly formed jaw retractors are prominent, laterally embraced by the corresponding interradial dilator double rows (Figs. 15D; 16 A, B, E) and

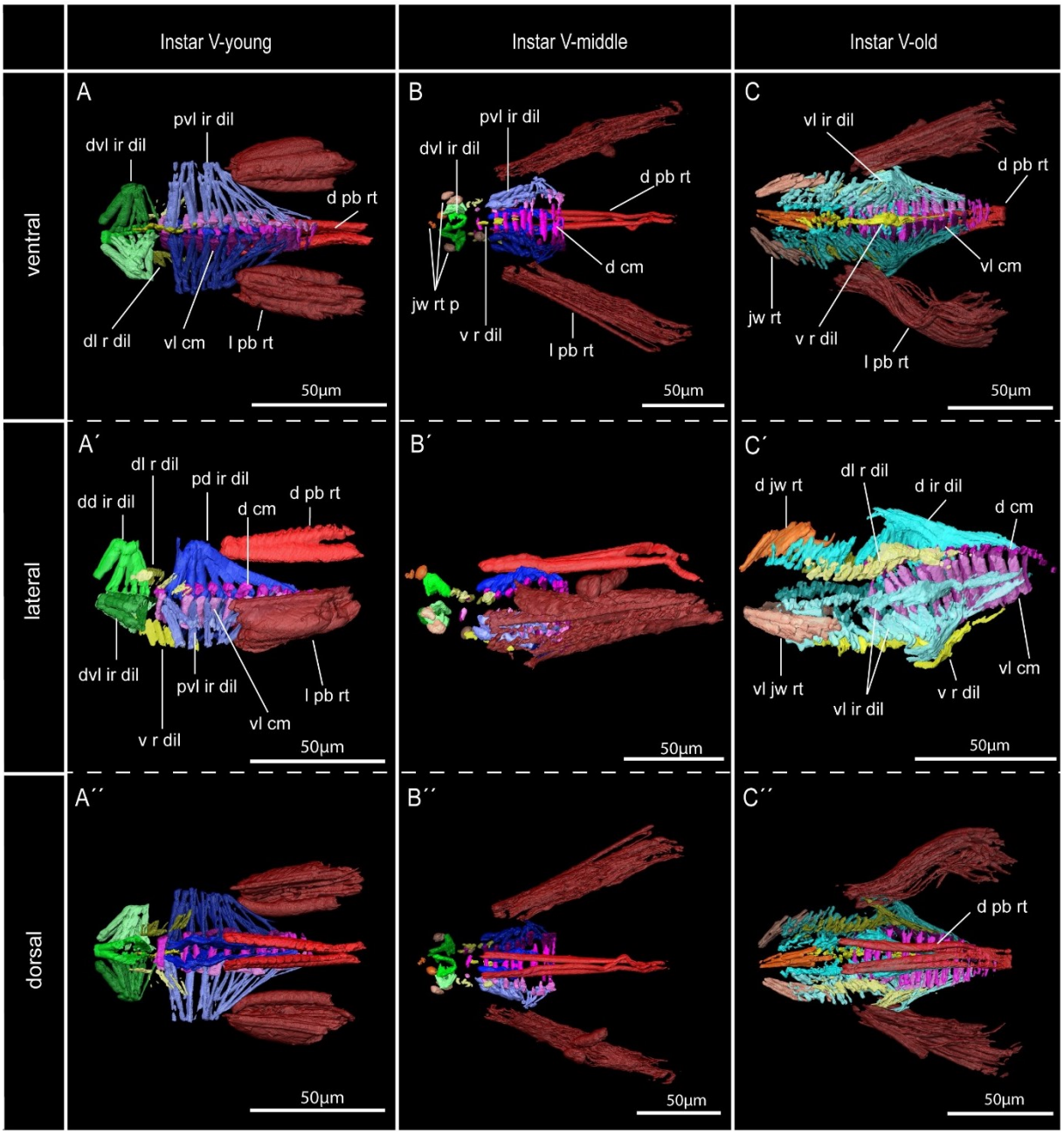

Figure 13: Positioning and configuration of the proboscis musculature during remodelling at instar V.

Reconstructions based on F-actin labelling of the remodelling of the proboscis musculature of a young, a middle-aged and an old (pre-moult) stage of instar V, shown in ventral (**A-C**), lateral (**A´-C´**) and dorsal (**A´´-C´´**) view, showing its triradiate symmetry. Muscle groups are colour coded: distal interradial dilator musculature (green), proximal interradial dilator musculature (blue), radial dilator musculature (yellow), constrictor musculature (magenta), proboscis retractor muscles (red) and the merged interradial dilator complex (light blue) in old instar V. (left column: **A-A´´**): proboscis musculature of young instar V with a similar configuration as the earlier instars. (middle column: **B-B´´**): The middle-aged instar V with degenerated proboscis musculature and the emergence of the paired jaw retractor muscle pioneer cells. (right column: **C-C´´**): The old stage of Instar V bears completely remodelled and compressed musculature. Note the positioning of the jaw retractors distally in between the muscle rows of the dilator musculature. The proximal dilator muscle fibers coil up inside the new cuticle because of the prolongation of existing muscle bundles (**C´**).

d cm, dorsal constrictor muscles; d ir dil, dorsal interradial dilator; dd ir dil, disto-dorsal interradial dilator; d jw rt, dorsal jaw retractor; dl r dil, dorsolateral radial dilator; d pb rt, dorsal proboscis

retractor; dvl ir dil, disto-ventrolateral interradial dilator; jw rt, jaw retractor; l pb rt, lateral proboscis retractor; pvl ir dil, proximo-ventrolateral interradial dilator; pd ir dil, disto-dorsal interradial dilator; v r dil, ventral radial dilator; vl cm, ventrolateral constrictor muscles; vl ir dil, ventrolateral interradial dilator; vl jw rt, ventrolateral jaw retractor

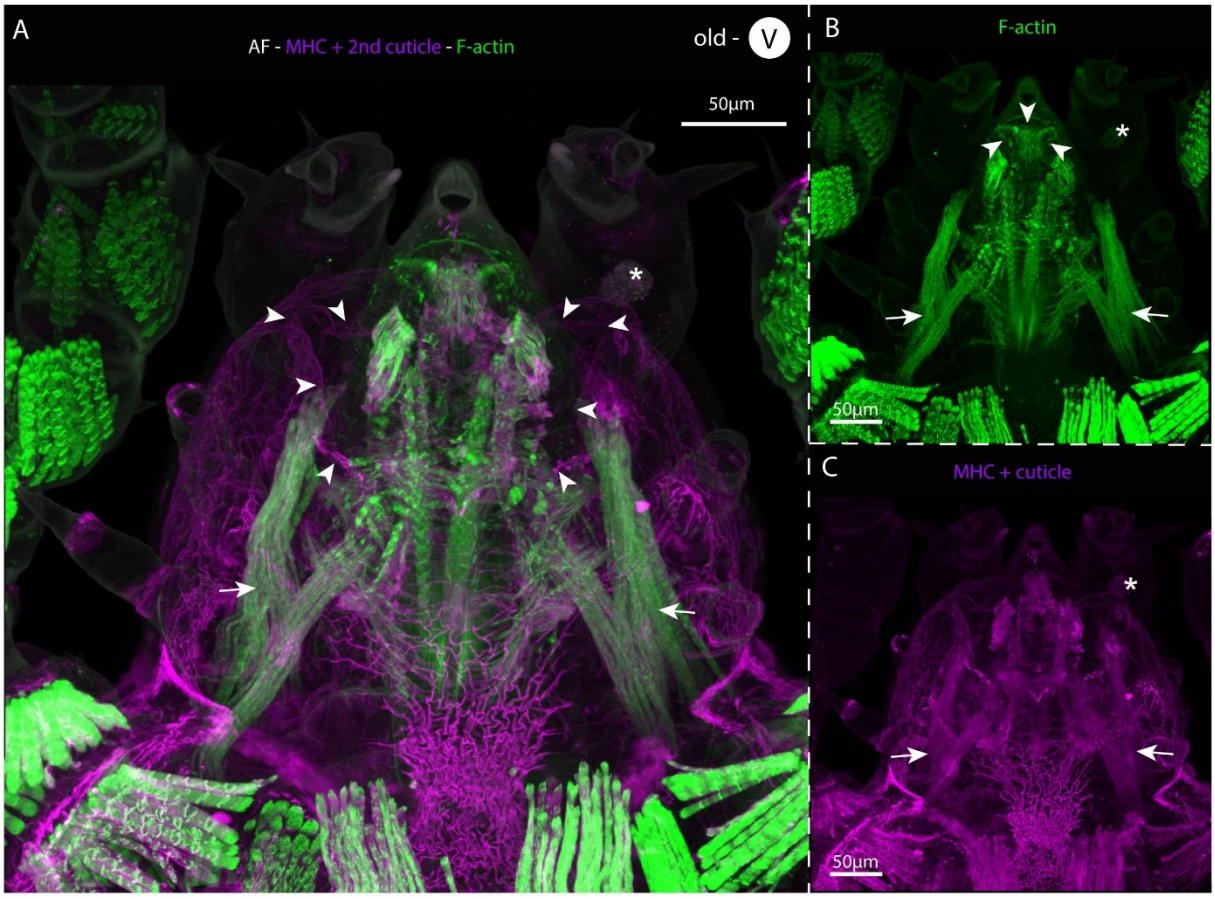

Figure 14: Folding of the remodelled proboscis within its old cuticle husk of an old stage of instar V. Volume renderings (MIP of CLSM scans) of an old stage instar V (pre-molt). F-actin labelling (green), myosin heavy chain immunolabelling and new cuticle (magenta) and autofluorescence of old cuticle (grey) in combination (**A**) and separately F-actin labelling (**B**) and MHC immunolabelling (**C**). The arrowheads (**A**) indicate the fold of the second cuticle, located at the base of the remodelled compressed proboscis. The arrowheads (**B**) indicate the formation of the jaws. The arrows indicate the lateral proboscis retractor muscles, with their distal ends located in the fold of the second cuticle. The asterisks mark atrophying cheliphore muscles, the remaining larval appendage musculature is already completely atrophied and the cuticle of larval appendages is empty.

AF, autofluorescence; MHC, myosin heavy chain (IHC)

extending proximally for approximately a quarter of the proboscis length (Figs. 15D; 16A). The constrictor muscles, the sole active antagonist to the dilators, are located in the proximal region of the proboscis (Figs. 15 A, C; 16 A, D, E), encircling the pharyngeal filter apparatus (the so-called oyster basket or ‘‘Reusenapparat’’). The ventro-lateral extrinsic retractor muscles undergo a significant growth from instar II to instar VI, becoming the most voluminous muscle groups of *P. litorale*, while the dorsal retractor maintains a moderate size (Figs. 15D; 16 A, E).

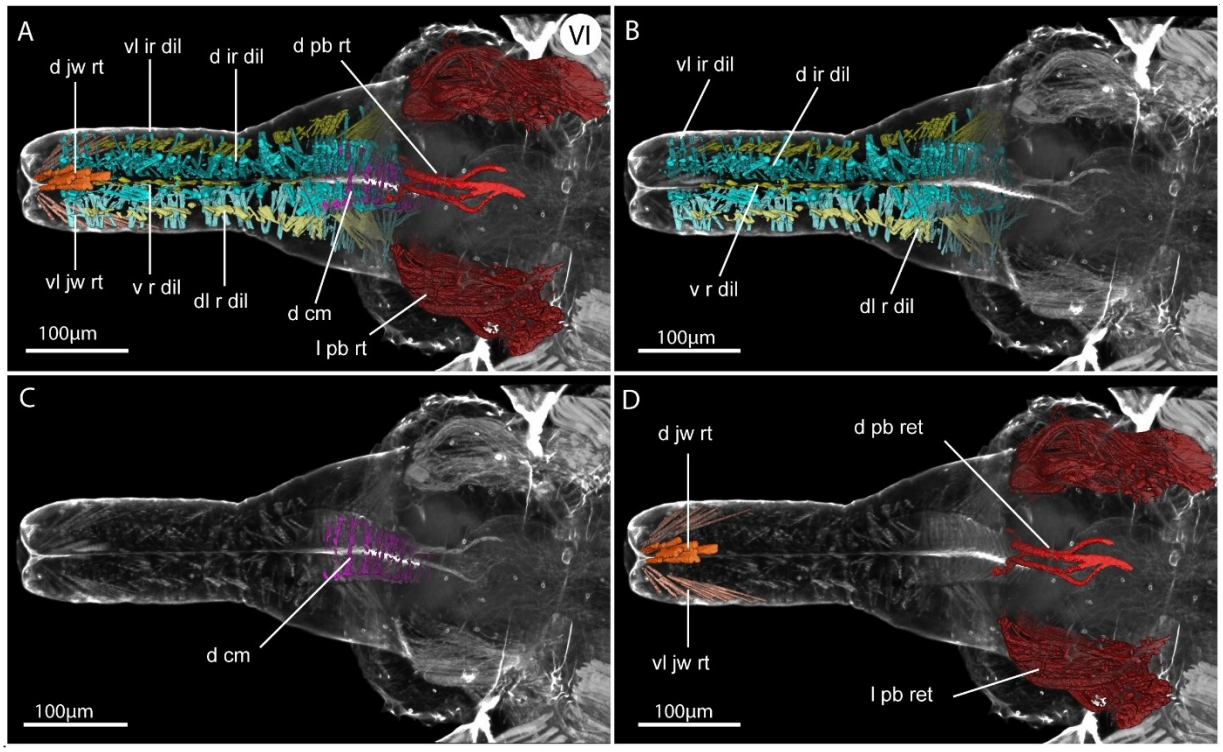

Figure 15: The proboscis musculature of the remodelled proboscis of instar VI.
Volume renderings (MIP of CLSM scans) with reconstructions based on F-actin labelling of the remodelled jaw, dilator, constrictor and extrinsic musculature at instar VI. With F-actin labelling (grey) and autofluorescence (grey) in dorsal view. Muscle groups colour coded: interradial dilator musculature (light blue), radial dilator musculature (yellow), constrictor musculature (magenta), proboscis retractor muscles (red), jaw retractor muscles (orange). (**A**): All muscle reconstructions shown in combination. (**B**): Reconstructions of pharynx dilators. Both pharynx dilators complexes spread along the entire length of the pharynx. Note that the proximal dilator muscle bundles are stretched and are no longer coiled up. (**C**): Reconstructions of pharynx constrictor musculature. The muscle rings are proximal positioned and arranged in succession for about a quarter of the proboscis length around the pharynx. (**D**): Reconstructions of proboscis and jaw retractor muscles. Note the volume of the lateral proboscis retractors, by comparison the dorsal proboscis retractor muscles are thin, both stretch from the base of the proboscis posterior through the cephalosoma. Jaw retractors are located at the distal end of the proboscis in between the primary pharynx dilator pairs.

d cm, dorsal constrictor muscles; d ir dil, dorsal interradial dilator; d jw rt, dorsal jaw retractor; dl r dil, dorsolateral radial dilator; d pb rt, dorsal proboscis retractor; l pb rt, lateral proboscis retractor; v r dil, ventral radial dilator; vl ir dil, ventrolateral interradial dilator; vl jw rt, ventrolateral jaw retractor

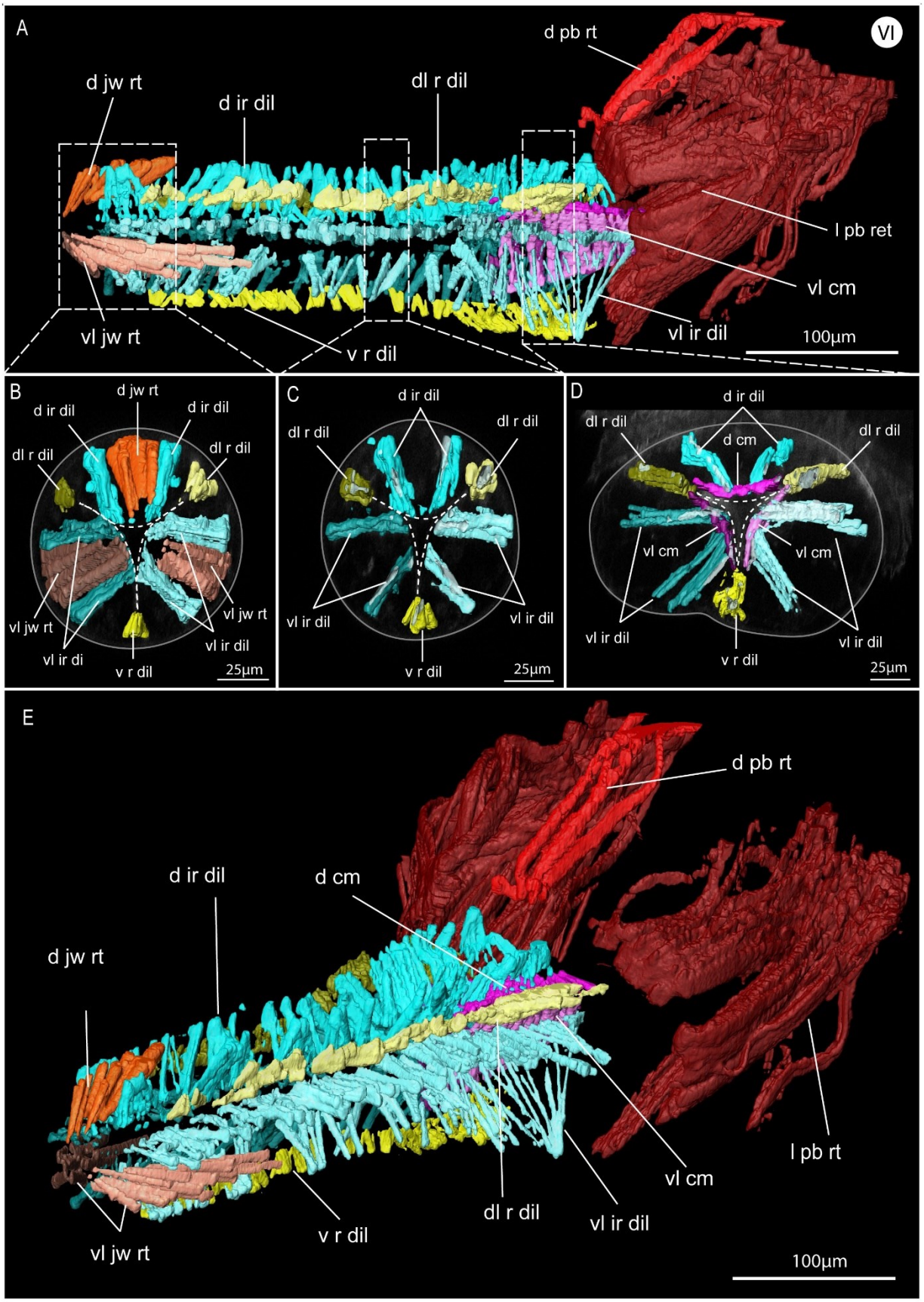

Figure 16: Positioning and configuration of the remodelled proboscis musculature of instar VI. Reconstructions of the remodelled proboscis musculature based on F-actin labelling of instar VI, in lateral (**A**) and dorsolateral frontal view (**E**), in combination with cross sections (**B-D**). Muscle groups colour coded: interradial dilator musculature (light blue), radial dilator musculature (yellow),

constrictor musculature (magenta), proboscis retractor muscles (red), jaw retractor muscles (orange). (**A**): Lateral view of the proboscis, dashed rectangles indicate location of cross sections. (**B-D**): Cross sections of the proboscis showing its triradiate symmetry, grey line indicating proboscis cuticle, dashed lines indicate location of the pharynx within the proboscis. (**B**): Distal cross section of the proboscis. The jaw retractors are located in between the interradial pharynx dilator pairs. (**C**): Middle cross section of the proboscis. Note that interradial pharynx dilators, consist of two dorsal and four ventrolateral muscle rows, in an interradial position along the proximo-distal axis of the pharynx, spanning from the pharynx to the inner wall of the proboscis cuticle. By contrast, radial pharynx dilators, consisting of one ventral and two dorsolateral muscle rows, located along the pharyngeal radii, spanning to the inner wall of the proboscis cuticle. (**D**): Proximal cross section of the proboscis. Each ring of pharynx constrictor muscles consisting of one dorsal and two ventrolateral muscles, located proximal around the pharynx stretching in between the pharyngeal radii. Note that each ring is located between the interradial dilator muscle fibers. (**E**): The dorsolateral frontal view facilitates a better understanding of three-dimensional configuration of the proboscis musculature at instar VI.

d cm, dorsal constrictor muscles; d ir dil, dorsal interradial dilator; d jw rt, dorsal jaw retractor; dl r dil, dorsolateral radial dilator; d pb rt, dorsal proboscis retractor; l pb rt, lateral proboscis retractor; vl cm, ventrolateral constrictor muscles; v r dil, ventral radial dilator; vl ir dil, ventrolateral interradial dilator; vl jw rt, ventrolateral jaw retractor

Discussion

The configuration and developmental sequence of the limb bud musculature and formation of the walking legs

During the anamorphic development of *P. litorale*, a functional walking leg pair emerges with each molt between the instars III and VII. It was already known that podomeres, joints and muscles had to develop prior inside of the limb buds (Vilpoux and Waloszek 2003; Alexeeva and Tamberg 2021) but the specific sequence of muscle development of the walking leg was unknown.

The hypothesis had been a successive development of the leg musculature from the proximal to the distal podomeres, similar to some crustaceans (Harzsch and Kreissl 2010), or even a simultaneous appearance of muscle pioneer cells. But the observed sequence is the simultaneous formation of muscle pioneer cells of the most proximal and the most distal muscles of the future walking leg, with a subsequent formation of the intermediate muscle pioneer cells. These mononucleated muscle pioneer cells form before any segmentation of the leg is visible. Concurrent with the occurrence of the intermediate muscles, the folding of the leg can be discerned for the first time. In what exact sequence the intermediate muscles appear, could not be determined completely. What is certain is that at very first the extrinsic leg muscles start to form, closely followed by the muscles within the first podomere (coxa2 levator and depressor) and within the penultimate podomere (claw levator and depressor).

Studies about the adult walking leg musculature of pycnogonids are rare (King 1973; Dencker 1974; Schram and Hedgpeth 1978; Schultz 1989). One comprehensive work about the locomotory mechanisms in Antarctic pycnogonids proposed the walking leg musculature of *Colossendeis australis* as typical for pycnogonids based on the comparison to some other long-legged Antarctic species (Schram and Hedgpeth 1978). These findings are consistent with the leg muscles of *N. brevirostre* described by Dencker (1974). And there are indeed many similarities with the walking leg musculature of *P. litorale* but also some key differences. With for pycnogonids comparatively short and thick podomeres, *P. litorale* has a modified walking leg, which is also reflected in its muscles. Coxa1 and coxa2 musculature are the same regarding attachment points and orientation in these three taxa. In *C. australis* the extrinsic leg muscles moving coxa1 are also oriented along a horizontal axis unlike the muscle group responsible for moving coxa2 where the muscles are rotated by 90 degrees into a vertical orientation, enabling protraction and retraction of the leg. All following muscles are again orientated along a horizontal axis in the three taxa. What also seems like a consistence in pycnogonid leg

musculature is the absence of propodus levator muscles within the tibia as well as the complete absence of muscles within the tarsus. As indicated by the available descriptions of pycnogonid leg musculature (King 1973; Dencker 1974; Schram and Hedgpeth 1978; Schultz 1989). The muscles within coxa2 and coxa3, however, are quite different in *P. litorale* to other species. Being symmetrical and confined to a single podomere in *C. australis* and *N. brevirostre*, in *P. litorale* the musculature of both podomeres is asymmetrical and some muscle fibers of the coxa3 levator stretch from coxa2 far into coxa3, supporting the femur levator located in coxa3. It is reasonable to assign these elongated muscle fibers with a different name as they are functionally a secondary group of femur levators, the term “coxa2-femur levator” is hereby proposed for this muscle. Describing its extending beyond the expected podomere boundaries. Muscles that extend over several podomeres were not yet reported in pycnogonids but are known in other chelicerate groups, such as Araneae and Acari (Schultz 1989). The femur levator within coxa3 is the most asymmetrical leg muscle as it is the only leg muscle located on just the anterior side of the podomere (Fig. 7 arrows), supported on both sides by the coxa3 levator (Fig. 7 arrowheads). This alteration of the “typical” pycnogonid leg musculature has probably something to do with the habitat and lifestyle of *P. litorale*. In contrast to many of its long-legged relatives, *P litorale* spends most of its time nearly stationary on rocky surfaces next to their prey as an ectoparasite (Schmidt and Bückmann 1971; Wilhelm et al. 1997). In this environment locomotion is secondary, most importantly is the ability to hold on to rocky substrate and or the feeding host. The alterations in leg and muscle morphology probably facilitates the fulfilment of this task.

The myogenetic pattern of the asymmetrical developing longitudinal trunk musculature and the discovery of the secondary longitudinal muscles

From instar IV onward, the emergence of a new trunk segment with each molt goes along with the development of longitudinal trunk musculature in the anteriorly adjacent segments.

According to the results of this study, the development of the longitudinal trunk musculature occurs in part asynchronous in the left and right body halves. In several specimens of instars IV and V, temporal differences between the developmental status of longitudinal muscles were observed. Muscle pioneer cells of the second ventral and dorsal longitudinal muscles in the cephalosoma give a strong MHC signal in one body half and none at all in the other (Fig. 8 D, E). Also, the depicted instar IV shows a difference in the development state of the first dorsal longitudinal muscles in the cephalosoma. Similar patterns of asynchronous muscle development were also observed in additional specimens. It can be assumed that longitudinal

muscles develop fully during the maturation of an instar stage. It also appears that the longitudinal muscles develop first in the ventral body side, as seen in (Fig. 8 B, B´).

The first ventral and dorsal longitudinal musculature of the cephalosoma develop during instar IV. The second longitudinal musculature of the cephalosoma and the first longitudinal musculature of the first trunk segment develop during instar V. Until now authors made no distinction between first and second longitudinal trunk musculature (Dencker 1974; Brenneis et al. 2023), probably because in adult pycnogonids these muscle groups are not easily distinguishable, due to their similar location and orientation. But during development there is a clear temporal difference in their formation as they develop in two separate instars.

Formation of anus dilator muscles and conformation of two distinct muscle groups

The anus dilator musculature starts forming in early- to middle-aged instar IV. F-actin can be labelled in these muscles at the end of instar IV (Fig. 9D), consistent with the results of Brenneis et al. (2023). At instar V, the anus dilators are well developed and the slit-like anus is discernible (Fig. 9E grey arrows), but according to previous studies, the ectodermal hindgut and endodermal mid-gut are still not connected to each other at this point (Alexeeva and Tamberg 2021). Alexeeva and Tamberg (2021) showed in histological sections that a border persists between mid- and hindgut throughout instar V with the opening of this border at instar VI. The anus musculature gives no indication at instar V that the digestive system is not yet connected to the hindgut. However, the visceral musculature of the midgut as visualized by F-actin labelling makes its border to the hindgut distinguishable in instar V. In late instar V and instar VI some of the dilator muscle fibers within the anal tubercle attach along the slit-like anus, and some fewer, later developing muscle fibers attach at a valve at the midgut-hindgut border. This valve has been previously described (Fahrenbach and Arango 2007; Alexeeva and Tamberg 2021). Furthermore, Fahrenbach and Arango (2007) mention a few muscle fibers between the valves and the inner wall of the anal tubercle, indicating the existence of two separate muscle groups. The results of this study, including the different developmental times of both sets, confirm this assumption.

New insights into the development of the proboscis muscles and the remodelling of the pharyngeal suction pump

The proboscis-associated musculature is the most complex muscle system in *P. litorale*. While the extrinsic musculature provides movability to the proboscis, the intrinsic musculature

functions as a suction pump (Dencker 1974; Fry 1965; King 1973; Wagner et al. 2017). In instars II to V, the pharynx is surrounded by two interradial pharyngeal dilator complexes, one distal, one proximal situated, which divide the pharynx into two functional parts.

The distal pharyngeal dilator complex has no muscular antagonists during instars II – V. Also after the remodelling of the proboscis and merging of the two dilator complexes, the distal part of the proboscis stays devoid of muscular antagonists at instar VI. This lack of active muscular antagonists to the pharyngeal dilator musculature in the distal part of the pycnogonid proboscis has led to some speculations in the past.

Dencker (1974) argues that in the proboscis of adult *N. brevirostre* the radial dilator muscles act as antagonists to the interradial dilator muscles. He proposes that the interradial muscles overstretch the pharyngeal antimeres to a convex form, thereby giving the cross-section of the pharynx the appearance of a bulbous triangle. With the contraction of the radial dilator muscles, the pharyngeal antimeres are stretched from a convex to a plane form, resulting in the cross-section of the pharynx taking on the appearance of a triangle. In accordance with this assumption the difference in the pharynx volume between the bulbous triangle and the plane triangle configuration is used to generate suction. Based on the results obtained by this study, this seems unlikely for the proboscis of the developmental stages of *P. litorale*. For one, up to instar IV the radial dilator muscles are small and seem underdeveloped. It is questionable whether they play any big a role in the first three instars at all, let alone act as the sole antagonist to the much more prominent distal dilator complex. Furthermore, the radial dilator complex is, in the first four instars, located more or less in between the two interradial dilator complexes. Which suggests that their role, up to the remodelling of the proboscis musculature at instar V, is to facilitate the transition of food from the distal pharynx compartment to its proximal compartment, through a somewhat peristaltic motion between the three dilator complexes.

A different proposal for the antagonist of the proboscis dilator complexes in pycnogonids gave King (1973). He argues that in adult pycnogonids the radial dilator muscles and interradial dilator muscles function together to change the trifoliate form (Y-shape) of the pharynx to a nearly triangular form, and that they are distally antagonised by the elastic, cuticularized foregut wall (i.e., the pharynx wall). This seem to be a more plausible explanation and aligns with the results and interpretation of this study. The pharynx of all scanned and studied proboscides were constricted. Before fixation, the specimens studied were treated with carbonated sea water to relax their muscles. Because the pharynx in its distal part was always Y-shaped, the forces keeping it in this form must be passive and not directly associated with musculature.

The proximal part the pharynx forms the pharyngeal filter, also known as “oyster basket’’ or the ‘‘Reusenapparat’’. The pharyngeal filter consists of elongated filter bristles which are attached to ring shaped ribs along the inner wall of the proximal pharynx. These ribs bear additional denticles and teeth (Fry 1965; Fahrenbach and Arango 2007; Wagner et al. 2017). The oyster basket has long been suspected to provide beside a filter function also a grinding mechanism for food uptake (Fry 1965), but the discussion about the precise functioning still persists to this day (Wagner et al. 2017).

At the location of the oyster basket, the proximal interradial dilator complex attaches to the pharyngeal wall. In between its muscle fibers, around the pharyngeal filter, the pharyngeal constrictor muscles are located. It appears that during development, the formation of additional constrictor ring muscles is accompanied by the formation of additional muscle fibers of the proximal interradial dilator complex. Whether this process is strictly synchronous is not clear, but there is at least a strong correlation. Prior to this study, the pharyngeal constrictor muscle complex was not reported for the first instar of pycnogonids (Alexeeva et al. 2017; Meisenheimer 1902) but recognized in adult pycnogonids by different authors (Fahrenbach and Arango 2007; King 1973; Dencker 1974; Wagner et al. 2017). The results of this study show well-developed constrictor muscles at instar II, which implies that they must develop at least in late instar I. It is also possible that they are already present after hatching and were overlooked in the past. They are the only muscular antagonist of the pharyngeal suction pump. The sequential arrangement of its circular-shaped muscles suggests the possibility of peristaltic contraction to facilitate the transportation of food further down to the esophagus. It is of course also possible that the elasticity of the pharynx is enough to withstand the pressure of the constrictor muscles and they do contract at once. What is certain, is that the constrictor muscles actively compress the whole region and are the antagonists to the proximal interradial dilator muscles in the first four instars.

For the contraction sequence of the distal and proximal pharyngeal dilator muscle during the first five instars several modes come into question. Either the contraction of both complexes is alternated and food is first sucked into the distal compartment and then through an interplay of proximal dilator contraction and distal dilator relaxation transported in the second compartment (the pharyngeal filter). Or they contract simultaneously, followed by a relaxation of first, the distal dilator and then a relaxation of the proximal dilator accompanied by a contraction of the constrictor muscles to press the food down the digestive tract. A simultaneous contraction and

relaxation of both pharyngeal dilator complexes would probably cause some of the food to be pushed back out of the pharynx, resulting in food loss and is therefore unlikely as contraction sequence.

At instar V, the remodelling of the proboscis leads to a drastic change of its musculature. During the remodelling phase all three dilator complexes degenerate in part, most of all the distal interradial dilator complex. This is probably due to the rearrangement of muscle attachment sites which especially concerns the distal interradial dilator complex. The remodelling of the proboscis musculature does not seem to happen solely over an epidermis growth between the muscle fiber attachment sites, but rather over a degeneration of existing muscles followed by a reorganization of attachment sites (probably by epidermis growth) and new muscle fiber formation. After remodelling, the distal interradial muscle fibers are uniformly arranged in rows along the interradial grooves of the pharynx. Also, the proximal interradial dilator muscles are reorganized, adding additional muscle fibers and growing in length and size but they still taper to one point inside of the cuticle. However, due to the proximity of the most proximal muscle fibers of the distal interradial dilator complex and the most distal muscle fibers of the proximal interradial dilator complex, both complexes seemingly merge and are no longer distinguishable from each other after remodelling.

To which point the musculature degenerates during remodelling is not completely clear, but the results show that at a point where distal and proximal interradial dilator complexes are still clearly divided from each other, already muscle pioneer cells of the jaw retractors form. The jaw retractors, fully developed at matured instar V, are also an indicator of the antagonistic role of the pharynx. These three distally located muscle groups are responsible for the opening of the three jaws. The jaw retractors have also no muscular antagonists, implying that their closing is made possible solely by the elasticity of the distal pharynx. Notably, Dencker (1974) distinguished two different jaw retractor muscle groups in *N. brevirostre*, one stretching into the most distal tip of the jaws and the other attaching behind them. In this work, however, it was decided against such a subdivision, because the individual muscle fibers are uniformly arranged next to each other.

One intriguing question is at what point during the development of instar V feeding is possible. In young instar V before the remodelling of the proboscis musculature it is quite safe to say that feeding is still possible. During the remodelling phase feeding is probably not possible due to how far the dilator musculature regresses. In pre-molting instar V, all muscle groups seem

functional and well-developed but spatially compressed. It is unlikely that feeding is possible in these late stages due to a lack of space within the proboscis, caused by the folded secondary cuticle and the significantly larger and compressed muscles compared to the beginning of instar V. Additionally, the molted distal pharynx of the old empty cuticle husk is constricted and probably prevents feeding (Fig. 12C arrowhead).

At instar VI, the proboscis musculature is eventually fully developed. Anterior to the pharyngeal filter the dilator musculature is uniformly arranged in rows, two interradial dilator muscle rows along each interradial grove and one radial dilator row along each radius of the pharynx. Around the pharyngeal filter the dilator musculature is elongated and the muscle fibers of each row taper together to one point inside of the cuticle. This prominence of dilator muscles at the proximal end of the proboscis in *P. litorale* differs from the described proboscis musculature of *N. spinosissima* and *N. brevirostre,* which is reported to have reduced dilators muscles in the region of the pharyngeal filter (Fahrenbach and Arango 2007; Dencker 1974). In their comprehensive study of proboscis morphology in several pycnogonid families by Wagner et al. (2017), they do not mention the distribution density of the pharynx dilator muscles. However, they do state that the length of the oyster basket of *P. litorale*, with a quarter of the proboscis length in adult specimens, is within the average (Wagner et al. 2017). The length of the oyster basket of *N. spinosissima* and *N. brevirostre* is notably longer with nearly half the length of the proboscis (Fahrenbach and Arango 2007; Dencker 1974). This suggests that the density of the dilator muscles is correlated with the length of the oyster basket. In other words, the shorter the filter apparatus, the more densely packed the muscle fibers are. On the other hand, the proboscis morphology of pycnogonids seems to be strongly correlated with the type of food ingested by the specimen (Wagner et al. 2017), indicating that the configuration of the proboscis musculature may also be influenced by this factor.

The results of this thesis, being first and foremost a morphological and not functional work, do not provide a comprehensive understanding of the detailed functioning of the suction pump in adult *P. litorale*. It seems plausible that peristaltic contractions of all pharyngeal dilator muscles, with additional support from the constrictor muscles as proximal antagonists, facilitate the transport of food down the digestive system. However, it cannot be ruled out that all dilator muscles contract simultaneously. For this to occur, the jaws of the proboscis probably must open and close repeatedly, forming a valve at the distal end of the proboscis, as they move through the suction cycles. Without additional functional investigation, the view of Dencker (1974) advocating radial and interradial pharyngeal dilator muscles to act antagonistically to

each other in the pharyngeal suction pump of adult pycnogonids, cannot be completely excluded. However, this mode of food uptake would use just a limited part of the available pharynx lumen for the creation of underpressure and therefore seems inefficient. By contrast, the function of the pharyngeal suction pump proposed by King (1973) with incorporation of one of the discussed muscle contraction sequences seem to be the more plausible solution in developing and adult *P. litorale*.

A clue to the founder cell model in Pycnogonida?

Since the first discovery of large mononucleate mesoderm cells termed muscle pioneers in grasshopper embryos (Ho, Ball and Goodman 1983) and the subsequent establishment of the founder cell model in *Drosophila* (Bate 1990; Rushton et al. 1995; Gunage et al. 2017; Baylies, Bate, and Gomez 1998; Schröter et al. 2004; Abmayr and Pavlath 2012; Campos-Ortega and Hartenstein 2013), the question of whether there is an overarching developmental mode of musculature in arthropods has been raised. Recently, two studies were able to confirm the fundamental steps of this mode of myogenesis in two isopods (Kreissl, Uber, and Harzsch 2008) and lobster larvae (Harzsch and Kreissl 2010), with the use of the monoclonal antibody 016C6. During development of the American lobster two elongated syncytial cords of precursors form along each of their thoracic limbs. These precursors probably initiated from mononucleate pioneers, then subdivide into - at first still connected - individual repeating muscle primordia (Harzsch and Kreissl 2010). In isopods, however, single mononucleated muscle pioneer cells are present in every podomere individually, which later develop into bi-, tri- and multinucleate syncyctia (Kreissl, Uber, and Harzsch 2008). Harzsch and colleagues conclude that the pattern of myogenesis displayed in the thoric limbs of the American lobster resembles probably the ancestral developmental process for crustaceans, being similar to the myogenetic pattern of the brine shrimp *Artemia salina* (Linnaeus, 1758) (Crustacea, Branchiopoda) and the ridgeback prawn *Sicyonia ingentis* (Burkenroad, 1938) (Crustacea, Decapoda) (Kreissl, Uber, and Harzsch 2008; Kiernan and Hertzler 2006). On the other hand, the myogenetic pattern displayed in isopod limbs has strong similarity with the muscle development of insects. However, it could not be determined if the development from mononucleated muscles pioneer cells to multinucleated muscle precursors takes place through the fusion of surrounding myoblasts as in insects (Abmayr and Pavlath 2012). This result led the authors to conclude that knowledge on crustacean myogenesis is still too limited to propose a homology between the myogenetic modes of crustaceans and insects (Kreissl, Uber, and Harzsch 2008). They also acknowledge that the substantial lack in knowledge about myriapod myogenesis must be addressed to

understand if the founder cell model is a synapomorphy of the Pancrustacea or if this mode of myogenesis originated earlier during arthropod evolution. They fail, however, to mention the equally large lack in knowledge about chelicerate myogenesis and that data about muscle development of an arthropod taxon outside the Mandibulata would give an even deeper insight in the evolution of arthropod myogenesis. The initial motivation for this master thesis was to address this lack of knowledge. The monoclonal antibody 016C6 was for the first time employed against MHCs in *P. litorale*. Because it was originally raised against a serum of locust MHCs (Kreissl, Uber, and Harzsch 2008), a control through HCR-FISH of MHCst was implemented. The high specificity of HCR-FISH through probe pairs and local amplification of hairpins (Schwarzkopf et al. 2021; Choi et al. 2018) enabled to verify that the antibody 016c6 predominantly cross-reacts indeed with MHCst in *P. litorale*. Beyond that, it helped to confirm that some of the weaker signals of the 016c6 labelling in the area of the midgut do not correspond to MHCst. Accordingly, the antibody 016c6 cross-reacts in *P. litorale* not exclusively, but mainly with MHC isoforms of striated musculature.

Using immunolabelling with the monoclonal antibody 016c6, cell nuclei of mononucleated muscle pioneer cells were visible in cross sections of the first limb bud at instar III as well as during the formation of longitudinal trunk musculature but were not distinguishable by HCR-FISH of MHCst probably due to immature mRNA being also labelled within the nucleus. These observations made for pioneer muscle cells of the longitudinal musculature suggests that the pioneers of each muscle form (almost) simultaneously as a group. The simultaneous emergence of a group of pioneer muscle cells of the longitudinal trunk muscles, which does not change in number, is different to the observed sequence of muscle pioneer cells of the limb muscles, where the number of pioneer cells in a given podomere increases over the course of muscle development. Notably, no unmistakable bi- tri- or multinucleated muscle precursor cells could be observed as in crustacean and insect limbs (Baylies et al. 1998; Kreissl, Uber, and Harzsch 2008; Harzsch and Kreissl 2010). Even in far-developed walking leg muscles within a limb bud shortly before molting, multinucleated syncyctia could not be identified with certainty. Instead, the observed mononucleated muscle pioneer cells of limb bud and longitudinal musculature seem to show a direct positional correspondence to later developing singular muscle fibers. The observation that singular muscle pioneer cells develop into singular muscle fibers coincides with the myogenesis of *Drosophila* (Gunage et al. 2017; Chal and Pourquié 2017). The difference to the described muscle formation of insects and crustaceans is that even in later stages of muscle development, when F-actin is already being detectable and the prospective muscle cells are elongated, each muscle pioneer cell seems to contain only a singular large

nucleus (Fig. 8 D-E´). In contrast, in crustaceans and insects the elongation and growth of each muscle cell happens by myoblast fusion and therefore over the gain of additional nuclei (Baylies et al. 1998; Kreissl, Uber, and Harzsch 2008; Harzsch and Kreissl 2010).
The late stage of mononucleated pioneer cells suggests that, if cell fusion happens at all during the myogenesis of *P. litorale* and therefore differentiated muscle cells are multinucleated, then this process must take place late and rather fast during muscle development after the growth and elongation of the muscle cells shown by the limb and longitudinal muscle formation.
Fahrenbach (1994) refers in his work about the fine structure of pycnogonid musculature, to the nuclei of somatic muscle cells with just one sentence, in which he implies that the nucleus is extending outside the cylinder of the muscle cell via a narrow neck. Unfortunately, this explanation is somewhat imprecise as Fahrenbach does not specify if he refers to the nucleus of one myofibril or the whole myofiber. The latter would imply that adult pycnogonid muscles are mononucleated, the former that they are multinucleated. For a more detailed description of the fine structure of pycnogonid muscles, the reader is directed to Fahrenbach (1994).

During instars IV and V, the muscle groups of the longitudinal trunk musculature (i.e., first and second longitudinal muscles of the cephalosoma, as well as first longitudinal muscles of the first trunk segment in instar V) are in different developmental states from each other, giving an opportunity to study muscles in different developmental stages in the same specimen.
The second longitudinal primordial muscles within the cephalosoma of instar V, consist seemingly of still mononucleated pioneer cells. While the first longitudinal muscles, located next to these second longitudinal muscles, are already giving a strong F-actin signal with no singular nuclei distinguishable around the muscle fibers. The first ventral and dorsal longitudinal muscle of the first trunk segment seem to be in a multinucleated state, but the obtained results make a reliable count of nuclei per muscle cell (muscle fiber) challenging.

What can be said with certainty is that in the leg podomeres, muscle pioneer cells form individually, like in isopods (Kreissl, Uber, and Harzsch 2008) and insect limbs and not along elongated cords of precursors as in the American lobster (Harzsch and Kreissl 2010). Also, HCR-FISH of MEF2 gives no indication of expression along elongated syncytial cords of precursors in *P. litorale*. This raises the question if the myogenesis mode of the American lobster is indeed the ancestral mode for crustaceans. If so, then the individual formation of muscles in limb podomeres would have evolved at least two times independently in arthropods.

However, the specification of mononucleated muscle pioneer cells at the start of myogenesis, previously reported only in crustaceans and insects, seems to be also present in pycnogonids. It represents therefore a promising candidate for the plesiomorphic state of the chelicerate lineage and perhaps even Euarthropoda. Given the muscle development described above during the anamorphic postembryonic developmental phase of *P. litorale* a more detailed examination of individual developing muscle cells of specific musculature, such as longitudinal, and limb muscles during the critical instars III-V, might provide a more comprehensive understanding of the myogenetic processes in this species. This could be achieved by the incorporation of different nuclear stains in combination with the used histochemical and IHC stains. In this thesis cell nuclei were labelled by DAPI, additionally in two experiments NucRed™ was tried out (App. 3). While NucRed™ did not give specific signals and was therefore not reported in this thesis, DAPI tends to give a more diffuse signal after a short period of time, in combination with the used methods, making it difficult to reliably count nuclei in differentiated muscle fibres. Beyond that, the persisting lack of knowledge regarding muscle formation in other chelicerates as well as in myriapods, must be addressed if the aim is to understand and reconstruct the ground pattern of myogenesis in Euarthropoda.

References

Abmayr, S.M. and Pavlath, G.K. "Myoblast fusion: lessons from flies and mice." Development 139, no. 4 (2012): 641-656.

Alexeeva, N., Bogomolova, E., Tamberg, Y. and Shunatova, N. "Oligomeric larvae of the pycnogonids revisited." Journal of Morphology 278, no. 9 (2017): 1284-1304.

Alexeeva, N. and Tamberg, Y. "Anatomical changes in postembryonic development of *Pycnogonum litorale*." Journal of Morphology 282, no. 3 (2021): 329-354.

Arnaud, F. and Bamber, R.N. "The Biology of Pycnogonida. " Advances in Marine Biology 24, (1988): 1–96.

Bate, M. "The embryonic development of larval muscles in *Drosophila*." Development 110, no. 3 (1990): 791-804.

Baylies, M.K., Bate, M. and Gomez, M.R. "Myogenesis: a view from *Drosophila*." Cell 93, no. 6 (1998): 921-927.

Behrens, W. "Larvenentwicklung und Metamorphose von *Pycnogonum litorale* (Chelicerata, Pantopoda)." Zoomorphology 104, no. 5 (1984): 266–79.

Bour, B.A., O'Brien, M.A., Lockwood, W.L., Goldstein, E.S., Bodmer, R., Taghert, P.H., Abmayr, S.M. and Nguyen, H.T. "*Drosophila* MEF2, a transcription factor that is essential for myogenesis." Genes & Development 9, no. 6 (1995): 730–41.

Brenneis, G., Bogomolova, E.V., Arango, C.P. and Krapp, F. "From egg to "no-body": an overview and revision of developmental pathways in the ancient arthropod lineage Pycnogonida." Frontiers in Zoology 14, no. 6 (2017): 1-22.

Brenneis, G., Frankowski, K., Maaß, L. and Scholtz, G. "The sea spider *Pycnogonum litorale* overturns the paradigm of the absence of axial regeneration in molting animals." Proceedings of the National Academy of Sciences 120, no. 5 (2023): e2217272120

Bruce, H. S., Jerz, G., Kelly, S., McCarthy, J., Pomerantz, A., Senevirathne, G., Sherrard, A., Sun, D.A., Wolff, C. and Patel, N.H. "Hybridization chain reaction (HCR) in situ protocol." protocols. io (2021): 1-10.

Campos-Ortega, J.A. and Hartenstein, V. "The embryonic development of *Drosophila melanogaster*." Springer Science & Business Media. (2013)

Chal, J. and Pourquié, O. "Making muscle: skeletal myogenesis in vivo and in vitro." Development 144, no. 12 (2017): 2104-2122.

Choi, H.M., Schwarzkopf, M., Fornace, M.E., Acharya, A., Artavanis, G., Stegmaier, J., Cunha, A. and Pierce, N.A. "Third-generation in situ hybridization chain reaction: multiplexed, quantitative, sensitive, versatile, robust." Development 145, no. 12 (2018): dev165753.

Dencker, D. "Das Skeletmuskelsystem von *Nymphon rubrum* Hodge, 1862 (Pycnogonida: Nymphonidae)." (1974).

Dietz, L., Dömel, J.S., Leese, F., Lehmann, T. and Melzer, R.R. "Feeding ecology in sea spiders (Arthropoda: Pycnogonida): what do we know?." Frontiers in zoology 15 (2018): 1-16.

Fahrenbach, W. H. 'Microscopic anatomy of Pycnogonida: I. cuticle, epidermis, and muscle." Journal of Morphology 222, no. 1 (1994): 33–48.

Fahrenbach, W.H. and Arango, C.P. "Microscopic anatomy of Pycnogonida: II. digestive system. III. excretory system." Journal of Morphology 268, no. 11 (2007a): 917–35.

Fry, W. G. " The feeding mechanisms and preferred foods of three species of Pycnogonida." Bulletin of the British Museum (Natural History) Zoology 12 (1965): 195-233

Giribet, G. and Edgecombe, G.D. "The phylogeny and evolutionary history of arthropods." Current Biology 29, no. 12 (2019): 592-602.

Gunage, R.D., Dhanyasi, N., Reichert, H. and VijayRaghavan, K. "*Drosophila* adult muscle development and regeneration." Seminars in cell and developmental biology, vol. 72, (2017): 56-66.

Harzsch, S. and Kreissl, S. "Myogenesis in the thoracic limbs of the American lobster." Arthropod Structure and Development 39, no. 6 (2010): 423-435.

Hedgpeth, J.W. "On the evolutionary significance of the Pycnogonida." Smithsonian Miscellaneous Collections 106, no. 18 (1947): 1-53.

Ho, R.K., Ball, E.E. and Goodman, C.S. "Muscle pioneers: large mesodermal cells that erect a scaffold for developing muscles and motoneurones in grasshopper Embryos." Nature 301, no. 5895 (1983): 66–69.

Jirikowski, G., Kreissl, S., Richter, S. and Wolff, C. "Muscle development in the marbled crayfish—insights from an emerging model organism (Crustacea, Malacostraca, Decapoda)." Development Genes and Evolution 220, no. 3-4 (2010): 89-105.

Jirikowski, G.J., Richter, S. and Wolff, C. "Myogenesis of Malacostraca–the "egg-nauplius" concept revisited." Frontiers in Zoology 10, no. 76 (2013): 1-27.

Kiernan, D.A. and Hertzler, P.L. "Muscle development in dendrobranchiate shrimp, with comparison with Artemia." Evolution & Development 8, no.6 (2006): 537–49.

King, P.E. "Pycnogonids." Hutchinson of London (1973)

Klementz, B.C., Brenneis, G., Hinne, I.A., Laumer, E.M., Neu, S.M., Hareid, G.M., Gainett, G., Setton, E.V.W., Simian, C., Vrech, D.E., Joyce, I., Barnett, A.A., Patel, N.H., Harvey, M.S., Peretti, A.V., Gulia-Nuss, M. and Sharma, P.P. "A novel expression domain of extradenticle underlies the evolutionary developmental origin of the chelicerate patella." Molecular Biology and Evolution 41, no. 9 (2024): msae188.

Kreissl, S., Uber, A. and Harzsch, S. "Muscle precursor cells in the developing limbs of two isopods (Crustacea, Peracarida): an immunohistochemical study using a novel monoclonal antibody against myosin heavy chain." Development Genes and Evolution 218, no. 5 (2008): 253-265.

Lin, M.H., Nguyen, H.T., Dybala, C. and Storti, R.V. "Myocyte-specific enhancer factor 2 acts cooperatively with a muscle activator region to regulate *Drosophila* tropomyosin gene muscle expression." Proceedings of the National Academy of Sciences 93, no. 10 (1996): 4623-4628.

Meisenheimer, J. " Beiträge zur Entwicklungsgeschichte der Pantopoden. I. Die Entwicklung von *Ammothea echinata* Hodge bis zur Ausbildung der Larvenform." Zeitschrift für wissenschaftliche Zoologie 72 (1902): 191-248.

Petrova, M. and Bogomolova, E. "Walking leg regeneration in the sea spider *Nymphon brevirostre* Hodge, 1863 (Pycnogonida)." Arthropod Structure and Development 77 (2023): 101310.

Pon, J.R. and Marra, M.A. "MEF2 transcription factors: developmental regulators and emerging cancer genes." Oncotarget 7, no. 3 (2015): 2297–2312.

Price, A.L. and Patel, N.H. "Investigating divergent mechanisms of mesoderm development in arthropods: the expression of Ph-twist and Ph-mef2 in *Parhyale hawaiensis*." Journal of Experimental Zoology Part B: Molecular and Developmental Evolution 310, no. 1 (2008): 24-40.

Schmidt, H.W. and Bückmann, D. "Beobachtungen zur Lebensweise von *Pycnogonum litorale* (Ström) (Pantopoda))." Oecologia 7, no. 3 (1971): 242–48.

Schram, F. R. and Hedgpeth, J. W. "Locomotory mechanisms in Antarctic pycnogonids." Zoological Journal of the Linnean Society 63, no. 1-2 (1978): 145-169.

Schröter, R.H., Lier, S., Holz, A., Bogdan, S., Klämbt, C., Beck, L. and Renkawitz-Pohl, R. "kette and blown fuse interact genetically during the second fusion step of myogenesis in *Drosophila*." Development 131, no. 18 (2004): 4501-4509.

Schultz, J.W. "Morphology of locomotor appendages in Arachnida: evolutionary trends and phylogenetic implications" Zoological Journal of the Linnean society 97, no. 1 (1989): 1-56.

Schwarzkopf, M., Liu, M.C., Schulte, S.J., Ives, R., Husain, N., Choi, H.M.T. and Pierce, N.A. "Hybridization chain reaction enables a unified approach to multiplexed, quantitative, high-resolution immunohistochemistry and in situ hybridization." Development 148, no. 22 (2021): dev199847.

Soler, C., Han, J., and Taylor, M.V. "The conserved transcription factor Mef2 has multiple roles in adult *Drosophila* musculature formation." Development 139, no. 7 (2012): 1270–75.

Subramanian, S.V. and Nadal-Ginard, B. "Early expression of the different isoforms of the myocyte enhancer factor-2 (MEF2) protein in myogenic as well as non-myogenic cell lineages during mouse embryogenesis." Mechanisms of development 57, no. 1 (1996): 103-112.

Tjønneland, A., Kryvi, H., Ostnes, J.P., and Økland, S. "The heart ultrastructure in two species of pycnogonids, and its phylogenetic implications. " Zoologica Scripta 14, no. 3 (1985): 215–19.

Tomaschko, K.-H., Wilhelm, E. and Bückmann, D. "Growth and reproduction of *Pycnogonum litorale* (Pycnogonida) under laboratory conditions." Marine Biology 129 (1997): 595-600.

Totland, G.K., and Kryvi, H. "The fine structure of the somatic muscles and their attachment to the cuticle in two species of Pycnogonida." Zoologica Scripta 15, no. 1 (1986): 69–72.

Vilpoux, K. and Waloszek, D. "Larval development and morphogenesis of the sea spider *Pycnogonum litorale* (Ström, 1762) and the tagmosis of the body of Pantopoda." Arthropod Structure & Development 32, no. 4 (2003): 349-383.

Wagner, P., Dömel, J.S., Hofmann, M., Hübner, J., Leese, F. and Melzer, R.R. "Comparative study of bisected proboscides of Pycnogonida." Organisms Diversity & Evolution 17, no. 1 (2017): 121–35.

Wilhelm, E., Bückmann, D. and Tomaschko, K.-H. "Life cycle and population dynamics of *Pycnogonum litorale* (Pycnogonida) in a natural habitat." Marine Biology 129 (1997): 601-606.

Appedices

Appendix 1: Buffers and solutions and their ingredients used in the experiments.

Buffers and solutions	**Ingredients**
PBS (phosphate-buffered saline)	1,86 mM NaH_2PO_4: 8,41 mM Na_2HPO_4; 175mM NaCl (pH 7,4)
PBTx	PBS + 0.5% Triton X-100 + 1.5% dimethyl sulfoxide
PBST	PBS with 0,1% Tween-20
5x SSCT	5x sodium chloride sodium citrate (SSC) with 0.1% Tween-20, RNase-free molecular grade water
detergent solution	1% SDS, 0,5% Tween-20, 50 mM Tris-HCL (pH 7,5), 1mM EDTA (pH 8,0) and 150 mM NaCl
hybridization buffer	30% formamide, 5x SSC, 9 mM citric acid (pH 6,0), 0,1% Tween-20, 50 µg/mL heparin, 1x Denhardt's solution, 10% dextran sulfate, RNase-free molecular grade water
amplification buffer	5x SSC, 0,1% Tween 20, 10% dextran sulfate, RNase-free molecular grade water
probe wash buffer	30% formamide, 5x SSC, 9mM citric acid (pH 6.0), 0,1% Tween 20, 50 µg/mL heparin, RNase-free molecular grade water

Appendix 2: Details on the staining reagents and mounting media used for fluorescent histochemistry, immunohistochemistry (IHC) and hybridization chain reaction RNA-fluorescent in-situ hybridization (HCR-FISH).

Staining reagent	Brand	Catalogue number	Concentration of stock solution	Employed laser lines	Labeling target/function
Fluorescent histochemistry					
DAPI (4′,6-diamidino-2-phenylindole)	Sigma-Aldrich	D9542	1mg/mL	405 nm	cell nuclei
Alexa Fluor™ 488 Phalloidin	Thermo Fisher Scientific	A12379		488 nm	F-actin
NucRed™ Dead 647 ReadyProbes™ Reagent	Thermo Fisher Scientific	R37113		633nm	cell nuclei
Immunohistochemistry antibodies					
monoclonal mouse 1AB 016c6	generated by Sabine Kreissl (Universität Konstanz)				MHC
monoclonal mouse 1AB 017c5	generated by Sabine Kreissl (Universität Konstanz)				MHC
Alexa Fluor™ 568 goat-anti-mouse 2AB	Thermo Fisher Scientific	A-11004	2 mg/mL	568 nm	
HCR-FISH hairpins					
B2-647	Molecular Instruments		3 µmol/L	633nm	MHCst
B2-594	Molecular Instruments		3 µmol/L	561nm	MHCst
B4-546	Molecular Instruments		3 µmol/L	561nm	MHCst
B5-647	Molecular Instruments		3 µmol/L	633nm	MEF2
Donkey anti-mouse 2AB (with B4 initiator)	Molecular Instruments				
Additional reagents					
Vectashield™	Vector Laboratories, Inc	H-1000	-	-	mounting medium
RapiClear™	SunJin Lab	RC149001	-	-	mounting medium
NGS (normal goat serum)	Thermo Fisher Scientific	PCN5000	-	-	blocking reagent

Appendix 3: Staining experiments and the staining reagents used.

Experiment Number	Nuclei stain	Fluorescent histochemistry	IHC – primary antibody	IHC – secondary antibody	HCR – hairpins
1	DAPI	Phalloidin	-	-	-
2	DAPI	-	mouse, clone 016c6	A568 goat-anti-mouse	-
2	DAPI	-	mouse, clone017c5	A568 goat-anti-mouse	-
2	DAPI	-	- (no primary control)	A568 goat-anti-mouse	-
3	DAPI	Phalloidin	-	-	-
4	DAPI	Phalloidin	mouse, clone 016c6	A568 goat-anti-mouse	-
5	DAPI	Phalloidin	mouse, clone 016c6	A568 goat-anti-mouse	-
6	DAPI	Phalloidin	mouse, clone 016c6	A568 goat-anti-mouse	-
6	NucRed™	Phalloidin	mouse, clone 016c6	A568 goat-anti-mouse	-
7	DAPI	Phalloidin	mouse, clone 016c6	A568 goat-anti-mouse	-
7	NucRed™	Phalloidin	mouse, clone 016c6	A568 goat-anti-mouse	-
8	DAPI	Phalloidin	mouse, clone 016c6	A568 goat-anti-mouse	-
9	DAPI	-	mouse, clone016c6	initiator-labeled donkey anti mouse	B4-A546 (MHC 016c6); B2-647(MHCst)
9	DAPI	-	-	-	B2-A647 (MHCst)
9	DAPI	-	-	-	B5-A647 (MEF2)
9	DAPI	-	-	-	B2-A594 (MHCst); B5-647 (MEF2)
10	DAPI	Phalloidin	mouse, clone 016c6	A568 goat-anti-mouse	-

Appendix 4: Sequences of the used probe pairs during HCR-FISH for the detection of myosin heavy chain (striated type 2) (MHCst) gene expression.

B2_Plit_MHC-ST_PP30_0						
Pair#	**Initiator**	**Spacer**	**Probe**	**Probe**	**Spacer**	**Initiator**
1	CCTCGTAAATCCTCATCA	aa	CGCCTCATCTTGTGTGCCATTCACA	TTGGCCCATGTCGTCGTCCGTTCGT	aa	ATCATCCAGTAAACCGCC
2	CCTCGTAAATCCTCATCA	aa	ATGTCTTGTTCCTATTCTGGAAGGC	TTTTCGTTAATGATGATCATTATGC	aa	ATCATCCAGTAAACCGCC
3	CCTCGTAAATCCTCATCA	aa	ATCAATGGTTTTATTCGTCGCCAGC	AATGTTTGGAAGCTATGCTAAAGTA	aa	ATCATCCAGTAAACCGCC
4	CCTCGTAAATCCTCATCA	aa	TTCTCAGATGCATCTGCACGTTCTT	TTCCTGGCTCTCAATTTTGCCAGAG	aa	ATCATCCAGTAAACCGCC
5	CCTCGTAAATCCTCATCA	aa	GTACGTCTTTATCTTTTGCTGGAGC	CTCCTCAGCCTCTTCGATCTGCCTC	aa	ATCATCCAGTAAACCGCC
6	CCTCGTAAATCCTCATCA	aa	TCCGGTAGTTCTTGGCAGCTTCAGA	CCAATTCCTTAACGCGACGTTCAGA	aa	ATCATCCAGTAAACCGCC
7	CCTCGTAAATCCTCATCA	aa	AGCGCTGCAGCCTCAGCTTCGTCGA	TTCTGGATGATCCTCTTGCCACCCT	aa	ATCATCCAGTAAACCGCC
8	CCTCGTAAATCCTCATCA	aa	CCATTCCCTTTCGCATCTTCTCCTG	TGACTTGCAATTCCTTGATCTGTTG	aa	ATCATCCAGTAAACCGCC
9	CCTCGTAAATCCTCATCA	aa	TTCGTCGGCAAGTCTTGCAGCATCT	CATTGCATGTTCTTGCTCGGCCCTA	aa	ATCATCCAGTAAACCGCC
10	CCTCGTAAATCCTCATCA	aa	TTTCTGGCTTCGTTCAGCATCTCGT	ATTGCCTTCTTTGCCTTCTCTTCAG	aa	ATCATCCAGTAAACCGCC
11	CCTCGTAAATCCTCATCA	aa	CTTCTAGCTTCCTCTTAGCCATCGA	GATCAGCCTGTAGGGTCTGCATCTC	aa	ATCATCCAGTAAACCGCC
12	CCTCGTAAATCCTCATCA	aa	CAGTTGATCGTGGGCTTCGGACAGT	TGAAGCATTGCTTGCAGTTAGTTCT	aa	ATCATCCAGTAAACCGCC
13	CCTCGTAAATCCTCATCA	aa	GCTTGTTCGAGGAGGGTACGGCTCT	CCCTCGGCTTGACGCCTTCCACGAT	aa	ATCATCCAGTAAACCGCC
14	CCTCGTAAATCCTCATCA	aa	TTCTTTCGGACATTCCTAACTGTTC	CCAATTCGCCGTGAAGAGCATTGCA	aa	ATCATCCAGTAAACCGCC
15	CCTCGTAAATCCTCATCA	aa	TTCGAGAGCTGCTTGCAAATCTTTG	GGCTTCGTCACGAGCACGGATCTCT	aa	ATCATCCAGTAAACCGCC
16	CCTCGTAAATCCTCATCA	aa	TGCGCTTCGGCGTTCGCCTTGTTGG	TTATTCTGGTATCGCTTCAAGTTCT	aa	ATCATCCAGTAAACCGCC
17	CCTCGTAAATCCTCATCA	aa	TGTCGCTCTCCAATTTCTTCTTCAT	GATCGAGAGCAATTTCGAGTTCGTT	aa	ATCATCCAGTAAACCGCC
18	CCTCGTAAATCCTCATCA	aa	GGCTTCCAAGCTCGCTTGCATCGAG	AAGTGCCTCTGCTTTGCCTTTGGCT	aa	ATCATCCAGTAAACCGCC
19	CCTCGTAAATCCTCATCA	aa	TTCTCGAACTCTTCCTCCTTCTCTT	ATGGCACGTTGGTGATTCTTACGCG	aa	ATCATCCAGTAAACCGCC
20	CCTCGTAAATCCTCATCA	aa	GAGAAAGTTCGAGCTGACTGCGGAG	TGCGACGGTCGATCTCTTGTCGCAC	aa	ATCATCCAGTAAACCGCC
21	CCTCGTAAATCCTCATCA	aa	TTCAGCCTCTTCTAACGCAGCTTGC	CTTGTTCTCTTCTTGCTCAAGAGCA	aa	ATCATCCAGTAAACCGCC
22	CCTCGTAAATCCTCATCA	aa	CTGATCTTCTCGAGCTCGTGTACCG	TCTTCCTTCTCCATCTCCAGACGCT	aa	ATCATCCAGTAAACCGCC
23	CCTCGTAAATCCTCATCA	aa	GATCCTTGACTTCGTCTGAGAGGTT	GTCCACCTTCGCCAAGTTGATCGAT	aa	ATCATCCAGTAAACCGCC
24	CCTCGTAAATCCTCATCA	aa	TTCTTGACTCTCCTCGTAATTGGCT	GTTCTCTCTCTGCAGAGCTTCGTAT	aa	ATCATCCAGTAAACCGCC
25	CCTCGTAAATCCTCATCA	aa	CTGCACTCTTTCTGCGATGCATCCA	AGCTTGAAGATCTCTGTGGAATAAT	aa	ATCATCCAGTAAACCGCC
26	CCTCGTAAATCCTCATCA	aa	TCCATTCGGCAATGGTCTTGTCGAA	CGGCAGCCAAATCGTCCACCTTTGC	aa	ATCATCCAGTAAACCGCC
27	CCTCGTAAATCCTCATCA	aa	CAATGCGTTAGCGCGATCTACTTCG	TTTCTGTCTCTTCTCGAGCGAACTT	aa	ATCATCCAGTAAACCGCC
28	CCTCGTAAATCCTCATCA	aa	CTCGATTTAGTCTTCTCCAGACCAC	GACATGTCTTCAATCTCTCCGGCCA	aa	ATCATCCAGTAAACCGCC
29	CCTCGTAAATCCTCATCA	aa	CCTCAGCCTCCTGTAATTTCATCTG	ATTTACCATTAAGTCCTTCGATAGT	aa	ATCATCCAGTAAACCGCC
30	CCTCGTAAATCCTCATCA	aa	CTCGAGAAAGACCTTCGCTTTCGTA	TTTTCTTTGCTTCTTCGAGTTCTTC	aa	ATCATCCAGTAAACCGCC

Appendix 5: Sequences of the used probe pairs during HCR-FISH for the detection of myocyte-enhancer-factor 2 (MEF2) gene expression.

B5_Plit_MEF2_PP24_1						
Pair#	**Initiator**	**Spacer**	**Probe**	**Probe**	**Spacer**	**Initiator**
1	CTCACTCCCAATC TCTAT	aa	GGTCATCCTGGCTCTTTTA CCGACC	CGACGCTCCGTGCCAC GAAGCCATC	aa	CTACCCTACAAATCC AAT
2	CTCACTCCCAATC TCTAT	aa	CTAGGATCCGGAGAATTTG ACGTCG	TTCGTATCGTATTCGAC GGGATGAG	aa	CTACCCTACAAATCC AAT
3	CTCACTCCCAATC TCTAT	aa	AACGATGTTCGGTCGCCGA TGCGGG	ATGACAGATGAGGATG ATGGACAGG	aa	CTACCCTACAAATCC AAT
4	CTCACTCCCAATC TCTAT	aa	TGGAGGTGATATCGGTTCG CTCTTT	ACGTATCACTACGTTGT CTTGACTG	aa	CTACCCTACAAATCC AAT
5	CTCACTCCCAATC TCTAT	aa	TGTTGTTGTTGATGATGAT GATGAT	CTAACAGGTAACGGTG AAGTAGATT	aa	CTACCCTACAAATCC AAT
6	CTCACTCCCAATC TCTAT	aa	AATGTGGCAAATTTGTTAC ACTGGC	GATGTTGTGGCGGTGG CGTAACCGA	aa	CTACCCTACAAATCC AAT
7	CTCACTCCCAATC TCTAT	aa	AGTAAGCGGTCCTTGGGA AGATGAC	ACTTAGTCCGGCAGCC TGAACTGCA	aa	CTACCCTACAAATCC AAT
8	CTCACTCCCAATC TCTAT	aa	CCGGTCGATAAACTCAGAT CAGCGG	CCATGAAGTAATCCGGC GGATCCTA	aa	CTACCCTACAAATCC AAT
9	CTCACTCCCAATC TCTAT	aa	AAGGCAAATTGGACGGAT GATGAAG	TTAGTTGGAAATCACTG TGGTACGT	aa	CTACCCTACAAATCC AAT
10	CTCACTCCCAATC TCTAT	aa	GTTGACGCCCGTGATATTA ACACTA	ATGATGTGGCTGCTGAT GAGGATAT	aa	CTACCCTACAAATCC AAT
11	CTCACTCCCAATC TCTAT	aa	CTCCCTGGGTTAGAAGATA AGTTAA	GACGGCACCGCACTTA AAGACACGA	aa	CTACCCTACAAATCC AAT
12	CTCACTCCCAATC TCTAT	aa	TGCTACTATTACTGCTGTTA ACAAC	TACTGATGGAAGTTGTT GTTCTACA	aa	CTACCCTACAAATCC AAT
13	CTCACTCCCAATC TCTAT	aa	GTTTGACATCGCATGATGT GGCGAC	GCCACTGCCGTTGTTAT GACTAACC	aa	CTACCCTACAAATCC AAT
14	CTCACTCCCAATC TCTAT	aa	CTCTGTCTACCGCAATTAC CGCCGA	TTCGACGACGGTATATG AATACGTA	aa	CTACCCTACAAATCC AAT
15	CTCACTCCCAATC TCTAT	aa	CTCCTCCAACTGGCGGACT ATTCTC	TTAGATCACTAGAACCA CCGTCACA	aa	CTACCCTACAAATCC AAT
16	CTCACTCCCAATC TCTAT	aa	CAAATGATGGACCGATGAA AGCGAA	CTTCGCATGAACATTCT TACTCGTC	aa	CTACCCTACAAATCC AAT
17	CTCACTCCCAATC TCTAT	aa	GGTGACGACTGATGATTGT AACCGT	GAACGTCTCGTGTCTGT TAAATCGT	aa	CTACCCTACAAATCC AAT
18	CTCACTCCCAATC TCTAT	aa	AAGAGTTTGGTCTTGGGCT CATATT	TGACATTCATGTCCAAT ATGTCTAC	aa	CTACCCTACAAATCC AAT
19	CTCACTCCCAATC TCTAT	aa	CAGAGTATTGTTATCTTGA CTGCTA	ATGAGCTGAACTTAAAT GAGAAGGT	aa	CTACCCTACAAATCC AAT
20	CTCACTCCCAATC TCTAT	aa	ATACCAACCGAAGTTACCG TTAATG	GGTGCGTAAGGTGACG GTACGCTGT	aa	CTACCCTACAAATCC AAT
21	CTCACTCCCAATC TCTAT	aa	TGTTCTGCGTGATGGAATT ACTCCG	AATTTTGATGGCTCACG TTTCCACC	aa	CTACCCTACAAATCC AAT
22	CTCACTCCCAATC TCTAT	aa	CTTGTGATACTTGGCTTCG GCACGA	CATCATCATTTCAAATT CTTCGTTA	aa	CTACCCTACAAATCC AAT
23	CTCACTCCCAATC TCTAT	aa	GGATCTGGACTTTCACTTC CTCCTT	GTCAAGACGTACTGTT CAGCCGAAT	aa	CTACCCTACAAATCC AAT
24	CTCACTCCCAATC TCTAT	aa	TATCGTTGTTGGTTCTACTT TCGTG	CGTCTTTCTTATTTAATG CCTCAAC	aa	CTACCCTACAAATCC AAT